Tumor-selective in vivo Growth Inhibitory Activities of siRNAs Targeting Kinetochore-Associated Protein 2

January 2019

Yukimasa MAKITA

Tumor-selective in vivo Growth Inhibitory Activities of siRNAs Targeting Kinetochore-Associated Protein 2

A Dissertation Submitted to
the Graduate School of Life and Environmental Sciences,
the University of Tsukuba
in Partial Fulfillment of the Requirements
for the Degree of Doctor of Philosophy in Biological Science
(Doctoral Program in Biological Sciences)

Yukimasa MAKITA

Table of Contents

Abstract

Kinetochore plays an important role in the precise segregation of chromosome during mitosis. Kinetochore-associated protein 2 (KNTC2) is a component of kinetochore sub-modules. It had been reported that the expression levels of KNTC2 are low in non-dividing normal cells and specifically upregulated in tumor tissues of various cancer patients. Some reports have indicated the relationship between KNTC2 and *in vivo* growth of tumor tissues. However, no anti-cancer drug had been developed targeting KNTC2. Therefore, I started this study to confirm the involvement of KNTC2 with *in vivo* growth of tumor tissues and show the possibility of developing siRNA drugs for cancer therapy.

In the first chapter, I selected highly potent siRNAs *in vitro* that were common for human KNTC2 and mouse *Kntc2*. Their IC_{50} values were less than 100 pM. These siRNAs were encapsulated into a lipid nanoparticle (LNP) for *in vivo* studies. KNTC2 siRNA-LNPs were intravenously administerd to otrhotopic tumor model mice of hepatocellular carcinoma (HCC). The expression levels of human KNTC2 and mouse *Kntc2* mRNAs in tumor tissues were significantly suppressed by KNTC2 siRNA-LNPs. KNTC2 siRNA-LNPs also increased the phosphorylation levels of histone H3 (HH3) at serine 10 in tumor tissues and suppressed the *in vivo* growth of HCC without inducing liver damages. These data demonstrated the tumor-selective *in vivo* growth inhibitory activities of KNTC2 siRNA-LNPs.

In the second chapter, I expanded the application of KNTC2 siRNA-LNP to lung cancer patient-derived tumor xenografts (PDXs). It had been reported that drug sensitivities of PDXs were more similar to tumor tissues of cancer patients compared

with conventional cancer cell lines. I firstly established three-dimensional (3D) culture systems of lung cancer PDXs (LC-45 and LC-60) because PDXs could not be maintained in two-dimensional culture systems. KNTC2 siRNA-LNP showed anti-tumor activities in 3D-culture system of LC-60 that was resistant to an approved drug, erlotinib. KNTC2 siRNA-LNP also showed anti-tumor activities in subcutaneous tumor model mice of LC-60 and LC-45 that was resistant to erlotinib. These results indicated that KNTC2 siRNA could be widely applied to lung cancer patients.

Taken together, I conclude that KNTC2 is a promissing target for patients with hepatocellular carcinoma and lung cancer. Phosphorylated HH3 at serine 10 was considered to be one of the pharmacodynamic markers for KNTC2 siRNA. These studies indicated a possibility of developing siRNA drugs for cancer therapy.

Abbreviations

ALT	Alanine transaminase
AST	Aspartate transaminase
CDCA1	Cell division associated 1
CDK1	Cyclin-dependent kinase 1
cDNA	Complementary deoxyribonucleic acid
CENP	Centromere protein
DPPC	Dipalmitoylphosphatidylcholine
dsRNA	Double-stranded RNA
HCC	Hepatocellular carcinoma
Hec1	Highly expressed in cancer protein 1
HH3	Histone H3
KD	Knockdown
KNTC2	Kinetochore-Associated Protein 2
KSP	kinesin spindle protein
LNP	Lipid nanoparticle
Luc	Luciferase
mRNA	Messenger ribonucleic acid
miRNA	MicroRNA
Ndc80	Nuclear division cycle 80
Nek2	NIMA-related kinase 2
OMe	*O*-methyl
PBS	Phosphate-buffered saline

PDX	Patient-derived tumor xenograft
PEG	Polyethylene glycol
PEI	Polyethylenimine
PLK1	polo-like kinase 1
pre-miRNA	Precursor miRNA
pri-miRNA	Primary miRNA
PS	Phosphorothioate
qPCR	Quantitative PCR
RISC	RNA-induced silencing complex
RNAi	RNA interference
shRNA	Short (or Small) hairpin RNA
siRNA	Small interferering RNA
SPC25	spindle pole body component 25 homolog

General Introduction

Kinetochore-associated protein 2

Precise segregation of chromosome during mitosis is essential to maintain the homeostasis of cells and organs. Missegregation of chromosome results in genome instability such as aneuploidy and leads to tumorigenesis[1]. In prometaphase, spindle microtubules extend from centrosome and bind to duplicated sister chromatids at the kinetochore region. The sister chromatids are aligned in the metaphase plate and segregated to the opposite poles during anaphase (Fig. 1).

Kinetochore consists of inner and outer sub-modules (Fig. 2). The inner kinetochore normally forms on highly repetitive DNA sequences and assembles into a specialized form of chromatin that persists throughout the cell cycle. The outer kinetochore is a proteinaceous structure with many dynamic components that assembles and functions only during mitosis[2]. The kinetochore has two main microtubule-interacting sub-modules, nuclear division cycle 80 (Ndc80) and Dam1. The Dam1 complex is thought to form a full or partial ring around microtubules, while the Ndc80 complex reaches out from the kinetochore with finger-like projections to contact the microtubule. The Ndc80 complex increases in copy number during anaphase, while the Dam1 subunits remain at a constant number[3].

Kinetochore-associated protein 2 (KNTC2), also called highly expressed in cancer protein 1 (Hec1)[4], is a component of Ndc80 complex[1] (Fig. 2). Human *KNTC2* mRNA is upregulated in tumor tissues of various cancer patients such as colorectal cancer[5], gastric cancer[5,6], breast cancer[7], non-small cell lung carcinoma[8], pancreatic cancer[9] and hepatocellular carcinoma[10]. In contrast, the expression level of mouse

KNTC2 protein was reported to be relatively low in normal liver where cells were not actively dividing[4]. Threfore KNTC2 was recognized as a potential target for cancer therapy[11]. Actually, some group had investigated the relationship between KNTC2 and tumor growth using retrovirus vector[12] or small molecules. However there is no approved drug targeting KNTC2 probably because it is difficult to develop molecules that are highly effective and specific to KNTC2. Retrovirus vector is not suitable for clinical development because of safety concerns. In this situation, I started to search for small interfering RNAs that were highly effective and specific to KNTC2.

Small interfering RNA

RNA-mediated gene silencing is an evolutionarily conserved immune system in which intracellular double-stranded RNAs (dsRNAs) are processed into small RNAs that suppress gene expression with complementary sequences[13]. In 1998, A. Fire *et al* investigated the mechanism of RNA-mediated gene silencing and discovered that injection of dsRNAs into *C. elegans* resulted in specific silencing of endogenous genes, which was called RNA interference (RNAi)[14]. RNAi was also confirmed in mammalian cells by Tuschl *et al.* in 2001[15]. A. Fire and C. Mello received the Nobel Prize in Physiology or Medicine 2006 for their discovery of RNAi.

Endogenous RNAi is triggered by microRNAs (miRNAs), that are transcribed as long primary miRNAs (pri-miRNAs) and processed into precursor miRNAs (pre-miRNAs) by Drosha (Fig. 3). These pre-miRNAs are then exported to the cytoplasm by the Exportin-5 and cleaved into small RNA duplexes of approximately 22 nucleotides by Dicer[16]. One strand of the mature miRNA is loaded into RNA-induced silencing complex (RISC) and cleaves homologous mRNAs.

Small interfering RNAs (siRNAs) are chemically syntesized dsRNAs (19-21 nucleotides) with overhanging 3' ends[15]. SiRNAs can be exogenously introduced into cells and enter the endogenous RNAi pathway at Dicer stage. The high specificity and efficiency of siRNA enabled us to easily validate molecular targets for anti-cancer drugs. For example, siRNAs targeting cell division associated 1 (CDCA1) and kinetochore associated 2 (KNTC2) were used *in vitro* to evaluate their involvement in the growth of lung cancer cell lines[8].

Issues that makes the clinical application of siRNA difficult are the vulnerability of siRNA to nuclease and immunogenicity. Several types of chemical modification[10], such as 2'-OMe, was examined to improve the stability of siRNAs or prevent immune-responses (Fig. 4). However, *in vivo* evaluation of KNTC2 siRNA had not been fully performed probably because there was no efficient *in vivo* delivery system for siRNA. Therefore I used a lipid nanoparticle (LNP) that was developed in-house for siRNA delivery.

Lipid nanoparticle

Several kinds of *in vivo* delivery systems, such as polyethylenimine (PEI)[17] and ligand-conjugate[18], have been developed for siRNA. Among them, LNPs (Fig. 5) were considered to be most promissing for cancer therapy[19,20]. Actually, siRNAs targeting the essential cell-cycle proteins polo-like kinase 1 (PLK1) and kinesin spindle protein (KSP) were validated *in vivo* using LNP[21]. These siRNAs showed knockdown activities and growth inhivitory activities in a orthotopic tumor model mice of hepatocellular carcinoma. Furthermore, first-in-human clinical trial was started in 2010 using LNP formulation of siRNAs targeting VEGF and KSP[22]. However, there was no report on

KNTC2 siRNA encapsulated into LNP. Therefore I started to use KNTC2 siRNA and LNP.

Objective of my studies

To confirm the involvement of KNTC2 in the growth of tumor tissues and show the possibility of developing KNTC2 siRNA drug for cancer therapy, I firstly selected highly potent KNTC2 siRNAs *in vitro* and encapsulated them into a LNP for *in vivo* studies. Anti-tumor activities of KNTC2 siRNA-LNP were investigated using orthotopic tumor model mice of hepatocellular carcinoma (chapter 1) and subcutaneous tumor model mice of lung cancer patient-derived tumor xenograft (chapter 2).

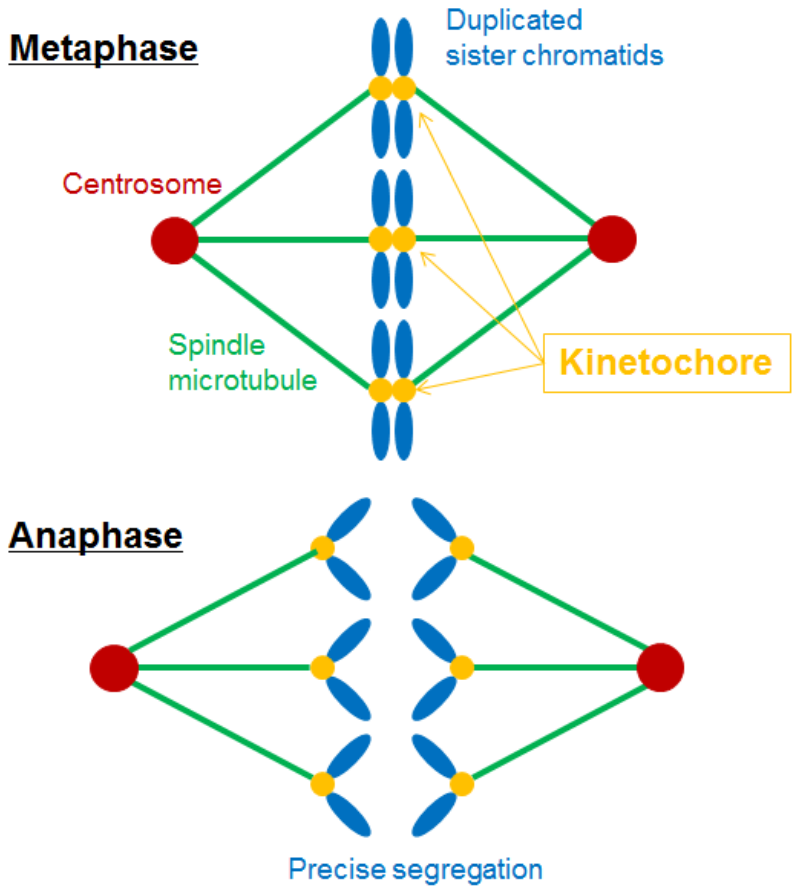

Figure 1 Segregation of sister chromatids during mitosis (modified from reference[1]). In metaphase (upper panel), spindle microtubules (green) extend from centrosome (red) and bind to duplicated sister chromatids (blue) at the kinetochore region (orange). These sister chromatids are aligned in the metaphase plate and precisely segregated to the opposite poles during anaphase (lower panel).

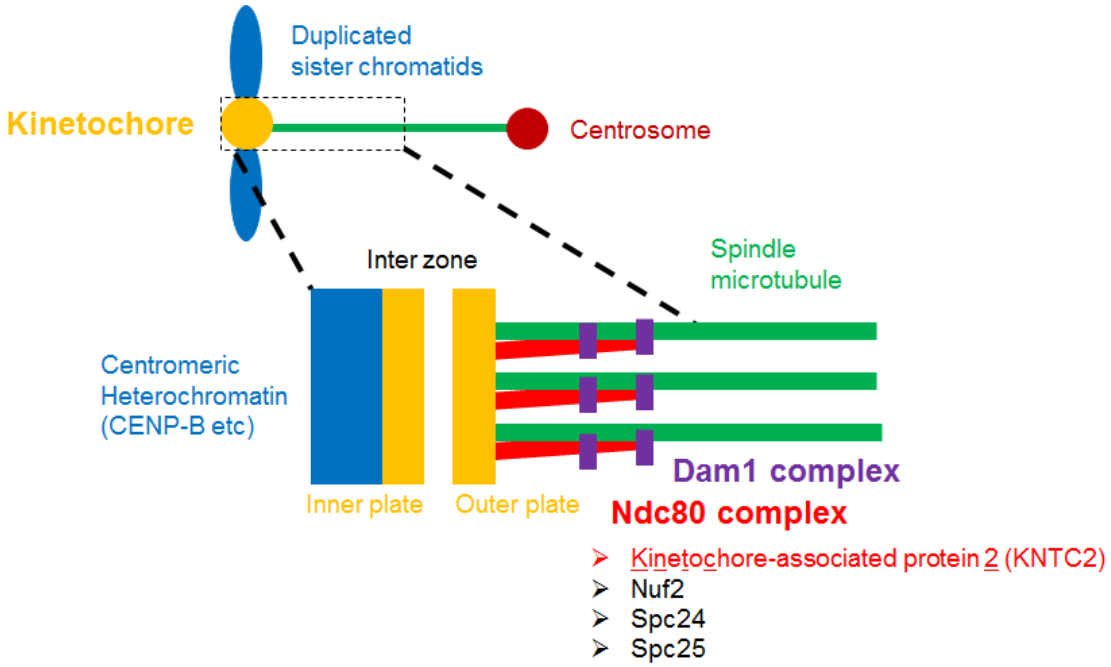

Figure 2 Structure of kinetochore (modified from reference[2]). The kinetochore is composed of several inner and outer plates (shown in yellow). Inner plate is a chromatin structure containing nucleosomes. Outer plate has attachment sites for the plus ends of microtubules (green). Dam1 complex (purple) and Ndc80 complex (red) are microtubule-interacting sub-modules. KNTC2 is a component of Ndc80 complex.

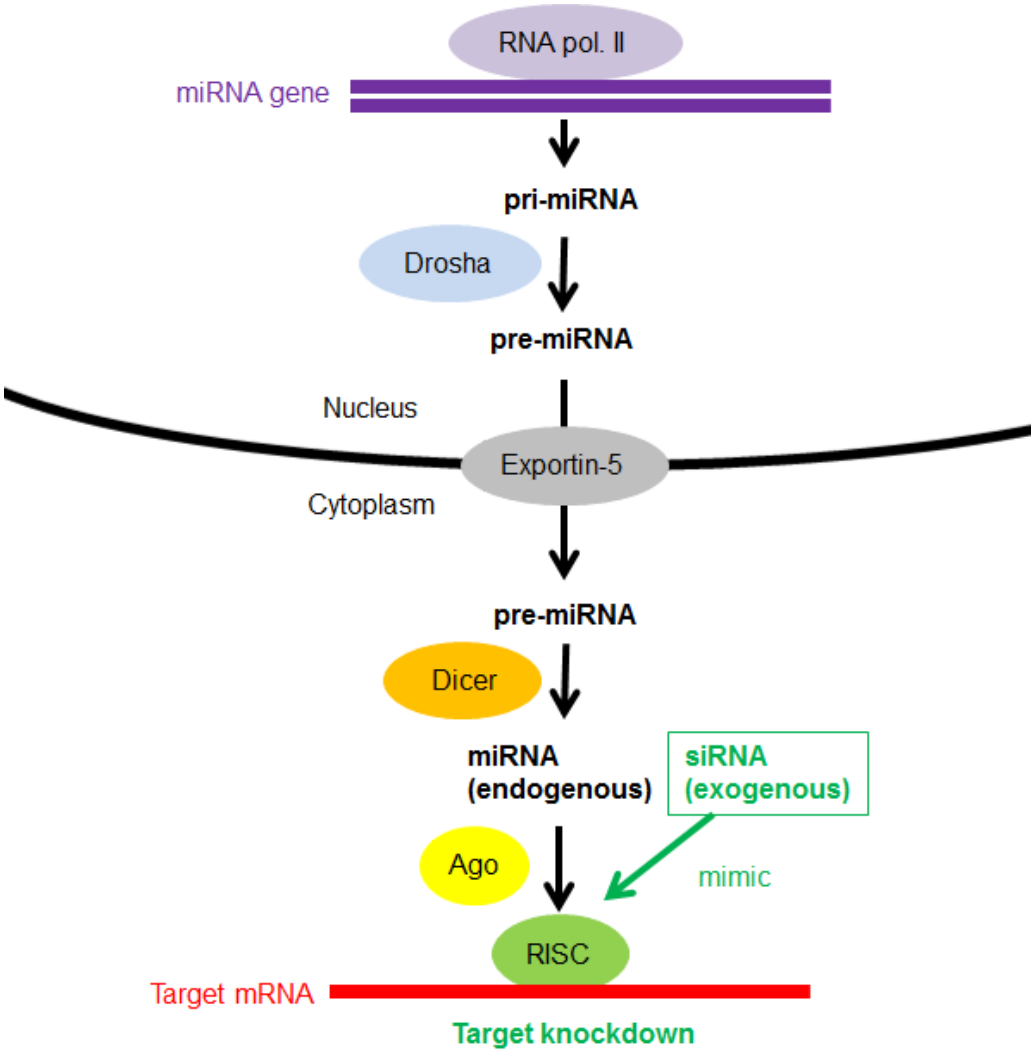

Figure 3 Endognous RNAi pathways and their use as tools for gene silencing (modified from reference[16]). Endogenous RNAi is triggered by pi-miRNAs that are processed into pre-miRNAs by Drosha (blue). Pre-miRNAs are exported to cytoplasm by Exportin-5 (gray) and cleaved into miRNA by Dicer (orange). One strand of mature miRNA is loaded into Ago (yellow) and forms RISC (green). Exogenous siRNAs (green) are loaded into Ago in the same way as miRNA.

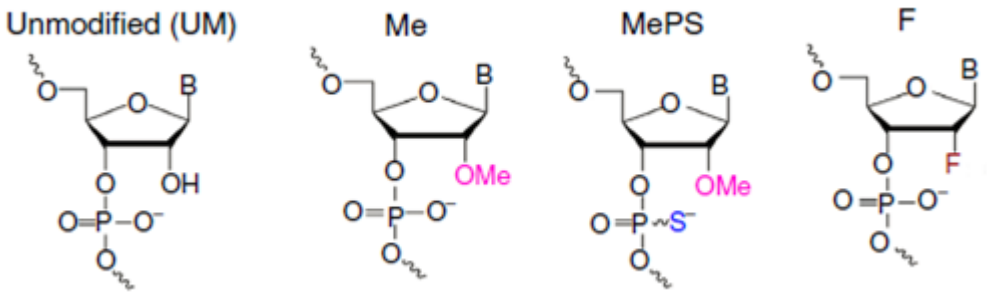

Figure 4 Chemical modifications of siRNA (modified from reference[10]). Chemical structures of modified nucleosides are shown. Me (pink), Methyl; S (blue), phosphorothioate; F (brown), Fluorine.

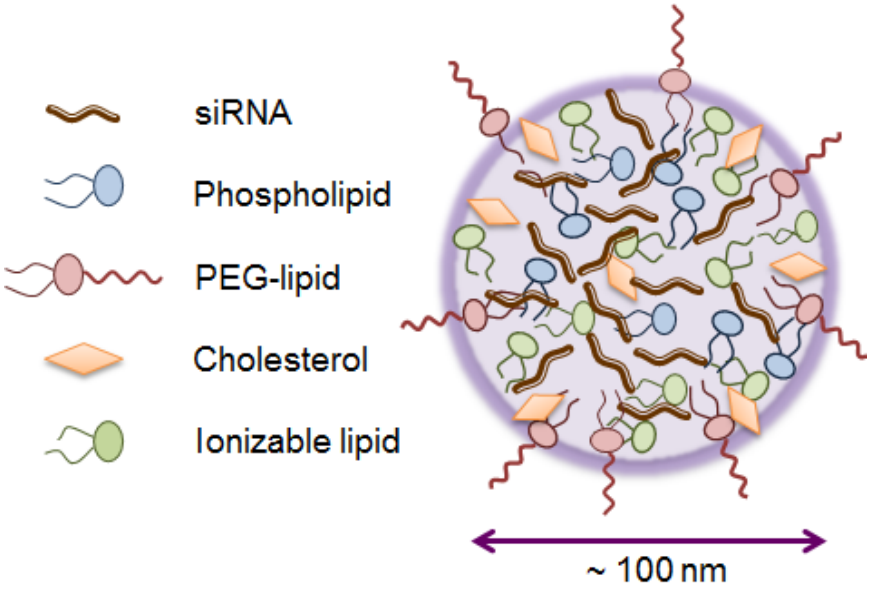

Figure 5 Schematic illustration of LNP (modified from reference[20]). LNPs encapsulating siRNAs mainly consist of ionizable lipid (green), phospholipid (blue), PEG-lipid (pink) and cholesterol (orange).

Chapter 1 : Anti-tumor activity of KNTC2 siRNA-LNP in orthotopic tumor model mice of hepatocellular carcinoma

Abstract

To clarify the involvement of KNTC2 in the growth of tumor tissues and develop siRNA drug for cancer therapy, I firstly selected highly potent KNTC2 siRNAs *in vitro* using human and mouse hepatocellular carcinoma cell lines. These siRNAs were encapsulated into a LNP for *in vivo* studies. Anti-tumor activities of KNTC2 siRNA-LNP were investigated using orthotopic tumor model mice of hepatocellular carcinoma. Single intravenous administration of KNTC2 siRNA-LNP specifically suppressed the expression levels of both human KNTC2 mRNA and mouse *Kntc2* mRNA in tumor tissues. Phosphorylation levels of histone H3 (HH3) at serine 10 in tumor tissues were increased by KNTC2 siRNA-LNP. Repeated administration of KNTC2 siRNA-LNP (twice a week) specifically inhibited the growth of tumor tissues without increasing the plasma AST and ALT levels. Their growth inhibitory activities were consistent with knockdown activities. These data strongly indicated that KNTC2 is a promising target for the treatment of HCC and that phosphorylated HH3 at serine 10 is one of the pharmacodynamic markers for KNTC2.

Introduction

Hepatocellular carcinoma (HCC) arises from a variety of disease states such as liver fibrosis[23], liver cirrhosis[24] and non-alcoholic fatty liver disease[25]. The risk factors of HCC are virus, alcohol, fungi, obesity and type II diabetes[26]. These factors lead to chronic inflammation, destruction and regeneration of hepatocytes or hepatic stellate cells resulting in genetic mutations and dysregulation of growth signals[27,28]. The etiology of HCC is so complicated that monotherapy is considered to be insufficient to cure all types of HCC.

Therapeutic options for HCC are surgical resection[29], liver transplantation[30], transarterial chemoembolization[31], radiotherapy[32], immunotherapy[33], interferon[34], iron chelator (deferasirox[35]) and molecular targeted agents, such as multi-kinase inhibitors (regorafenib[36], sorafenib[37]), anti-glypican-3 antibody (codrituzumab[38]), mTOR inhibitors (everolimus[39]) and anti-VEGF antibodies (bevacizumab[40], ramucirumab[41]). Those therapies show some clinical benefits for several types of HCC patients but their therapeutic effects are limited. HCC is still the second[42] or third[43] cause of cancer-related death in the world. Therefore, new drugs with different mechanism of actions are desired for HCC patients to improve their survival rates.

As described in the general introduction, kinetochore-associated protein 2 (KNTC2) plays an important role in chromosome segregation during mitosis[4]. Its expression levels are specifically upregulated in tumor tissues of various cancer patients including HCC[44]. Small molecules targeting KNTC2 protein (TAI-1, TAI-95) inhibited the *in vitro* growth of several HCC cell lines without inhibiting the growth of normal cell lines[44]. TAI-1 and TAI-95 also demonstrated *in vivo* growth inhibitory activity in a

subcutaneous HCC model of Huh-7 cells. However, there is no follow-up report on the relationship between KNTC2 and *in vivo* growth of HCC. It is still unclear whether KNTC2 is widely involved in the growth of HCCs. In addition, their mechanism of actions are not yet fully understood *in vivo*.

To further investigate the relationship between KNTC2 and *in vivo* growth of HCC and confirm its tumor-selectivity, I firstly selected highly efficient KNTC2 siRNA and encapsulated them into a lipid nanoparticle. Their knockdown efficiencies, pharmacodynamic marker, growth inhibitory activities and hepatotoxicities were evaluated in orthotopic HCC model mice of Hep3B-luc cells.

Materials and Methods

Chemical modification of siRNAs

All siRNAs used in this study were chemically modified with 2'-*O*-methyl ribonucleotide to prevent immune responses[45]. Their sequences were listed in Table 1. Luc#1 was originally designed for firefly luciferase gene[15] and used as the negative control for *in vitro* studies. NC#1 was designed as a mismatch control of Luc#1 and used for *in vivo* studies.

In vitro selection of KNTC2 siRNAs

Hep3B (human hepatocellular carcinoma cell line) and Hepa-1c1c7 (mouse liver hepatoma cell line) were purchased from American Type Culture Collection (ATCC, Manassas, VA). These cells were seeded in 96-well plates (BD Biosciences, San Jose, CA), cultured overnight and transfected with KNTC2 siRNAs (56 fM to 10 nM) using DharmaFECT1 (Thermo Fisher Scientific, Waltham, MA). Twenty four hours after the transfection, total RNA was extracted from cells and reverse-transcribed using Cells to Ct kit (Thermo Fisher Scientific). Copy number of each mRNA was measured by quantitative PCR method using Real-Time PCR System (Thermo Fisher Scientific). Primers and probes were listed in Table 2. IC_{50} value of each KNTC2 siRNA was calculated using Prism 5.0 (GraphPad, La Jolla, CA).

Encapsulation of siRNAs into lipid nanoparticles

KNTC2 siRNAs were encapsulated into lipid nanoparticles using microfluidic devices, Asia modules (model no. 210, Syrris, Royston, UK). LNP was composed of

3-((5-(dimethylamino) pentanoyl)oxy) -2,2-bis (((3-pentyloctanoyl)oxy)methyl)propyl 3-pentyloctanoate (WO2016021683), dipalmitoyl phosphatidylcholine (NOF Corporation, Tokyo, Japan), cholesterol (Avanti Polar Lipids, Inc., Alabaster, Alabama) and GS-020 (NOF Corporation) at the molar ratio of 60%, 10.6%, 28% and 1.4%, respectively. Particle size and polydispersity index (PdI) of LNPs were measured by dynamic light scattering using Zetasizer Nano ZS (Malvern Instruments, Malvern, UK). The ratio of siRNA entrapment was calculated using Ribogreen (Thermo Fisher Scientific, Waltham, MA) and 2% Triton X-100 as described elsewhere[46]. Briefly, LNPs were dissolved in 1% Triton X-100 to release the siRNAs. The concentrations of siRNA prior to and following the dissolution were calculated by applying Ribogreen (final 0.25%) and measuring the fluorescence of Ribogreen using a spectrofluorometer, Envision (Excitation, 485 nm and Emission, 535 nm) and Envision software (version 1.13.3009.1409, PerkinElmer, Inc., Waltham, MA, USA).

Establishment of Hep3B cells stably expressing firefly luciferase gene

Human hepatocellular carcinoma cell line, Hep3B was purchased from ATCC and cultured in EMEM (Thermo Fisher Scientific) containing 2% L-Glutamine and 10% fetal bovine serum (ATCC). Fluc gene fragment originally encoded by pGL3-Control vector (Promega, Madison, WI) was inserted into pAcGFP1-N In-Fusion Ready vector (Clontech, Mountain View, CA) and introduced into Hep3B cells. Clone number Ef2 stably expressing Fluc gene (Hep3B-luc) was isolated in a medium containing 400 μg/ml geneticin (Thermo Fisher Scientific).

Orthotopic tumor model of hepatocellular carcinoma

C.B-17/Icr-scid/scid (SCID) mice (female, 5 or 6 weeks old) were purchased from CLEA (Kanagawa, Japan) and acclimatized. Hep3B-luc cells (3×10^5 cells) were washed with HBSS and centrifuged. The cell pellet was mixed with approximately equal volume (3 μl) of Matrigel (BD, Franklin Lakes, NJ) using MICROMAN (Gilson, Middleton, WI). The cell suspension (6 μl) was inoculated into the liver (left lobe) of SCID mice under anesthesia. Tumor growth was assessed by measuring the luminescence from Hep3B-luc cells using IVIS Spectrum (PerkinElmer, Waltham, MA). All experiments were approved by the Institutional Animal Care and Use Committee in Takeda Pharmaceutical Company Limited (approval number AU-00020234).

Evaluation of anti-tumor activity using *in vivo* imaging system

Eleven days after the inoculation, SCID mice with Hep3B-luc cells were divided into groups by the values of luminescence and body weight (N=5). KNTC2 siRNA-LNP (1 mg/kg) was intravenously administered twice a week during the test period. Tumor growth was monitored by IVIS Spectrum (PerkinElmer) until five days after the last administration. Values of the final measurement were statistically analyzed by Dunnett's test. Growth inhibitory rates (%) were calculated using the formula (1-Y/X)×100; X, tumor weight of control group; Y, tumor weight of test group. Photographs of dissected tumor tissues were taken after the final measurement.

Measurement of the hepatotoxicity

Just after the final measurement of anti-tumor activity, blood was collected from the tail vein of mice under anesthesia (N=5). Plasma AST and ALT levels were measured by

DRI-CHEM 3500 (FUJIFILM, Tokyo, Japan).

Measurement of the *in vivo* knockdown activities by qPCR

KNTC2 siRNA-LNP (1 mg/kg) was intravenously administered to HCC model mice eighteen or nineteen days after the transplantation (N=3). Two days after the single administration, tumor tissue and normal liver were separately dissected from mice. Total RNA was extracted using TRIzol reagent (Thermo Fisher Scientific) and reverse-transcribed using superscript VILO cDNA synthesis kit (Thermo Fisher Scientific). Copy number of each mRNA was measured as described above. Values were statistically analyzed by Dunnett's test.

Immunohistochemistry

Administration of KNTC2 siRNA-LNP was performed in the same manner as above mentioned (N=2). Two days after the single administration, tumor tissue and normal liver were dissected together from mice. These samples were fixed with 10% Formalin Neutral Buffer Solution (Wako) and paraffin embedded. Tissue sections (5 μm) were deparaffinized and autoclaved in Real Target Retrieval solution (Agilent, Santa Clara, CA) for immuno-stimulation. Primary and secondary antibodies were listed in Table 3. They were diluted in normal goat serum blocking solution (Vector Laboratories, Burlingame, CA). Tissue sections were mounted on slides using VECTASHIELD Mounting Medium with DAPI (Vector Laboratories). Images were acquired by NanoZoomer Digital slide scanner (Hamamatsu Photonics, Shizuoka, Japan).

Results

In vitro screening of KNTC2 siRNAs

To find highly potent KNTC2 siRNAs, I designed approximately 250 siRNAs and measured their *in vitro* KD activities against human *KNTC2* mRNA in Hep3B-luc cells. The IC_{50} values of selected eleven siRNAs (#1 to #11) were between 3 pM to 58 pM (Table 4). Among the eleven siRNAs, four siRNAs (#1 to #4) showed relatively high KD activity against mouse *Kntc2* mRNA in Hepa1c1c7 cells. Their IC_{50} values were 94 pM, 50 pM, 19 pM and 62 pM (Table 4).

In vivo knockdown activities of KNTC2 siRNAs-LNP

Knockdown activities of KNTC2 siRNAs (#1 and #3) were evaluated in orthotopic HCC model mice of Hep3B-luc. Single intravenous administration of KNTC2 siRNA-LNP (1 mg/kg) significantly suppressed the expression levels of human KNTC2 mRNAs by 74% (KNTC2#1) or 78% (KNTC2#3), respectively. In contrast, NC#1-LNP (negative control) did not significantly suppress the expression level of human KNTC2 mRNA (Fig. 6A). Mouse *Kntc2* mRNAs were also suppressed by 52% or 75% at the same dosage (Fig. 6B). Lower dosage of KNTC2 siRNA-LNP (0.3 mg/kg) also suppressed the expression levels of human KNTC2 mRNAs by 55% or 68%, respectively (Fig. 6C). Mouse *Kntc2* mRNAs were suppressed by 49% or 68% at the same dosage (Fig. 6D).

Pharmacodynamic marker of KNTC2 siRNAs-LNP.

I next investigated a potential pharmacodynamic marker for KNTC2. Phosphorylation levels of histone H3 (HH3) at serine 10 in tumor tissues of HCC seemed to be increased by KNTC2 siRNAs-LNP (1 mg/kg) two days after the single intravenous administration (Fig. 7A, B and C). NC#1-LNP (negative control) did not seem to increase the phosphorylation levels of HH3 (Fig. 7D). In addition, phosphorylated HH3 seemed to be fragmented by KNTC2 siRNAs-LNP indicating that KNTC2 siRNA-LNP induced apoptosis (Fig. 7B, C).

In vivo growth inhibitory activity of KNTC2 siRNAs-LNP

Anti-tumor activities of KNTC2 siRNA-LNPs were evaluated at the same dosage as described above. Repeated administration (twice a week) of KNTC2 siRNA-LNP (1 mg/kg) significantly inhibited the *in vivo* growth of Hep3B-luc cells as measured by IVIS (Fig. 8A, E) and tumor weight (Fig. 8B). NC#1-LNP (negative control) did not significantly inhibit the *in vivo* growth of Hep3B-luc cells. The growth inhibitory rates were 94% (KNTC2#1) or 99% (KNTC2#3) as calculated by tumor weight (Fig. 8B). These values were consistent with the appearance of tumor tissues (Fig. 8F). Body weights of mice were not significantly changed by the repeated administration of KNTC2 siRNA-LNP at the dosage of 1 mg/kg (Fig. 8G). Lower dosage of KNTC2 siRNA (0.3 mg/kg) also significantly inhibited the *in vivo* growth of Hep3B-luc cells as measured by IVIS (Fig. 8C) and tumor weight (Fig. 8D). The growth inhibitory rates were 54% (KNTC2#1) or 87% (KNTC2#3) as calculated by tumor weight (Fig. 8D).

Hepatotoxicity of KNTC2 siRNA-LNPs in orthotopic HCC model mice

In parallel with the anti-tumor activity, we evaluated the hepatotoxicity of KNTC2 siRNA-LNP by measuring the plasma AST and ALT levels. These levels were increased in control groups (PBS and NC#1) probably because orthotopic tumor tissues damaged the surrounding hepatic cells (Fig. 9A, B). In contrast, repeated administration of KNTC2 siRNA-LNP (1 mg/kg, twice a week) significantly lowered the plasma AST and ALT levels indicating that they suppressed the tumor growth without inducing hepatotoxicity.

Discussion

To confirm the relationship between KNTC2 and *in vivo* growth of HCC, I firstly selected highly potent siRNAs for human and mouse KNTC2. These siRNAs were encapsulated into a LNP and administered to orthotopic HCC model mice. Their KD efficiency, pharmacodynamic marker, growth inhibitory activity and hepatotoxicity were evaluated.

Among the four siRNAs that showed relatively high KD efficiencies *in vitro*, I selected KNTC2#1 and KNTC2#3 for *in vivo* study because KNTC2#2, KNTC2#3 and KNTC2#4 were designed very closely within the gene structure of KNTC2. In contrast, KNTC2#1 was designed apart from KNTC2#3. Both of these separately-designed siRNAs inhibited the *in vivo* growth of orthotopically inoculated Hep3B-luc cells (Fig. 8). Their growth inhibitory activities were consistent with their KD activities (Fig. 6). In addition, the specificities of these KD and growth inhibitory activities were confirmed by the inability of NC#1. These data strongly indicated that KNTC2 was involved in the *in vivo* growth of orthotopically inoculated Hep3B-luc cells.

In vivo growth inhibitory activity of KNTC2#1 was lower than that of KNTC2#3 at the dosage of 0.3 mg/kg (Fig. 8C, D), which was consistent with their *in vitro* and *in vivo* KD activities (Table 4 and Fig. 6C, D). *In vivo* growth inhibitory activity might not be detected by other siRNAs whose *in vitro* KD activities were much lower than KNTC2#1. Generally, administration of high dose siRNA and lipid nanoparticle (LNP) faces a risk of unexpected adverse events, such as off-target effect[47] and toxicity of cationic lipids[48]. Therefore lowering the dosage of siRNA and LNP by selecting highly potent siRNAs *in vitro* was considered to be crucial to demonstrate *in*

vivo growth inhibitory activity without causing adverse events.

KNTC2 siRNA-LNP increased the phosphorylation levels of HH3 at serine 10 in the tumor tissues (Fig. 7). Phosphorylation of HH3 at serine 10 is reported to be correlated with chromosome condensation during mitosis and meiosis[49]. Previous report demonstrated that anti-KNTC2 antibody disturbed mitosis and induced a fragmentation of nuclei[4]. In my *in vitro* studies, KNTC2 siRNA induced misalignment of chromosome in Hep3B-luc cells and G2/M cell cycle arrest (Figs. 10-11). Taken together, it was estimated that KNTC2 siRNA-LNP disturbed the mitosis of Hep3B-luc cells in tumor tissues and induced G2/M cell cycle arrest resulting in the chromosome condensation and accumulation of phosphorylated HH3.

Compared to subcutaneous HCC models[50], orthotopic HCC models were considered to be more suitable for the simultaneous evaluation of anti-tumor activity and hepatotoxicity because tumor tissues were mixed with normal liver (Fig. 8F). I selected KNTC2 siRNAs that suppressed not only human *KNTC2* mRNA but also mouse *Kntc2* mRNA to simultaneously investigate the effect of KNTC2 siRNA on tumor tissue and normal liver (Table 4). Hepatotoxicity of KNTC2 siRNA-LNP was not detected at the therapeutic dosage (1 mg/kg) suggesting the safety of targeting KNTC2 (Fig. 9).

Repeated administration of KNTC2 siRNAs-LNP significantly lowered the plasma AST and ALT levels in the orthotopic HCC model mice of Hep3B-luc (Fig. 9). AST and ALT are released mainly from damaged hepatocytes[51]. Therefore, it was speculated that a portion of normal hepatocytes were damaged by the aggressive proliferation of tumor tissues and that tumor shrinkage by KNTC2 siRNAs-LNP led to the protection of normal hepatocytes and decrease of plasma AST and ALT levels (Figs.

8-9).

In conclusion, I demonstrated the anti-tumor activities of KNTC2 siRNAs-LNP in an orthotopic HCC model of Hep3B-luc cells at the dosage of 0.3 and 1 mg/kg. I also clarified the increase and segmentation of phosphorylated histone H3 in tumor tissues treated with KNTC2 siRNAs-LNP. Hepatotoxicity was not detected at the therapeutic dosage (1 mg/kg). These data strongly indicated that KNTC2 is a promising target for the treatment of HCC and that phosphorylated HH3 at serine 10 is one of the pharmacodynamic markers for KNTC2.

Tables and Figures

Table1 List of chemically modified siRNAs. Small cases "r", "d" and "s" indicate ribonucleotide, deoxy-ribonucleotide and phosphorothioate modification, respectively. Underline indicates 2'-*O*-methyl ribonucleotide.

Luc siRNA (Luc#1)	
Sense	5'-r(CUUACGCUGAGUACUUCGA)-dTsdT-3'
Antisense	5'-r(UCGAAGUACUCAGCGUAAG)-dTsdT-3'
Negative control siRNA (NC#1)	
Sense	5'-r(CUUACCCUCAGUUGUUCGA)-dTsdT-3'
Antisense	5'-r(UCGAACAACUGAGGGUAAG)-dTsdT-3'
KNTC2 siRNA (KNTC2#1)	
Sense	5'-r(UGGAGGAUACUUUAGAACA)-dTsdT-3'
Antisense	5'-r(UGUUCUAAAGUAUCCUCCA)-dTsdT-3'
KNTC2 siRNA (KNTC2#2)	
Sense	5'-r(AUAGUCAACUUGGUAUAUU)-dTsdT-3'
Antisense	5'-r(AAUAUACCAAGUUGACUAU)-dTsdT-3'
KNTC2 siRNA (KNTC2#3)	
Sense	5'-r(UAGUCAACUUGGUAUAUUU)-dTsdT-3'
Antisense	5'-r(AAAUAUACCAAGUUGACUA)-dTsdT-3'
KNTC2 siRNA (KNTC2#4)	
Sense	5'-r(CAACUUGGUAUAUUUUCCA)-dTsdT-3'
Antisense	5'-r(UGGAAAAUAUACCAAGUUG)-dTsdT-3'
KNTC2 siRNA (KNTC2#5)	
Sense	5'-r(GUCUAGAGUCGUUGAGAAA)-dTsdT-3'
Antisense	5'-r(UUUCUCAACGACUCUAGAC)-dTsdT-3'
KNTC2 siRNA (KNTC2#6)	
Sense	5'-r(GACAUUGAGCGAAUAAAUC)-dTsdT-3'
Antisense	5'-r(GAUUUAUUCGCUCAAUGUC)-dTsdT-3'

Table1 (continued)

KNTC2 siRNA (KNTC2#7)	
Sense	5'-r(CUAGUUGUGCAAACCACGA)-dTsdT-3'
Antisense	5'-r(UCGUGGUUUGCACAACUAG)-dTsdT-3'
KNTC2 siRNA (KNTC2#8)	
Sense	5'-r(AUAUAUCCAUAGUGAAUAA)-dTsdT-3'
Antisense	5'-r(UUAUUCACUAUGGAUAUAU)-dTsdT-3'
KNTC2 siRNA (KNTC2#9)	
Sense	5'-r(GACAUUGAGCGAAUAAAUU)-dTsdT-3'
Antisense	5'-r(AAUUUAUUCGCUCAAUGUC)-dTsdT-3'
KNTC2 siRNA (KNTC2#10)	
Sense	5'-r(UAAACAAACCGACAUCUGA)-dTsdT-3'
Antisense	5'-r(UCAGAUGUCGGUUUGUUUA)-dTsdT-3'
KNTC2 siRNA (KNTC2#11)	
Sense	5'-r(CAGACAUUGAGCGAAUAAA)-dTsdT-3'
Antisense	5'-r(UUUAUUCGCUCAAUGUCUG)-dTsdT-3'

Table 2 List of species specific qPCR primers and probes. Small case "d" indicates deoxy-ribonucleotide.

Human *KNTC2*	Sequence
Fw primer	5'-d(GAGGTACATAAACTTGAGCCCTGTATT)-3'
Rev primer	5'-d(TGCTGAGAATTCCAAAGGTTATGA)-3'
Probe	5'-d(TGGCACCAGCCTCGGGATTAAACTTAA)-3'
Human *ACTB*	**Sequence**
Fw primer	5'-d(CCTGGCACCCAGCACAAT)-3'
Rev primer	5'-d(GCCGATCCACACGGAGTACT)-3'
Probe	5'-d(ATCAAGATCATTGCTCCTCCTGAGCGC)-3'
Mouse *Kntc2*	**Sequence**
Fw primer	5'-d(GAATAAAAAGAGGCATCTGGAGGATAC)-3'
Rev primer	5'-d(CCTCCTTCAGCATCCTCACAGT)-3'
Probe	5'-d(CAACTGAACACCATGAAAACGGAAAGCAA)-3'
Mouse *Actb*	**Sequence**
Fw primer	5'-d(CACTATTGGCAACGAGCGG)-3'
Rev primer	5'-d(TCCATACCCAAGAAGGAAGGC)-3'
Probe	5'-d(TCCGATGCCCTGAGGCTCTTTTCC)-3'

Table 3 List of antibodies used in immunohistochemistry.

Primary antibody	**Clone**	**Host**	**Maker**	**Number**	**Dilution**
Anti-phospho-Histone H3 (Ser10) XP	D2C8	rabbit	Cell Signaling	#3377	1/200
Anti-alpha-Tubulin	DM1A	mouse	Sigma	T6199	1/200
Secondary antibody	**Clone**	**Host**	**Maker**	**Number**	**Dilution**
Anti-rabbit IgG (H+L), Alexa Fluor 568 conjugate	poly.	goat	ThermoFisher	A11036	1/200
Anti-mouse IgG (H+L), Alexa Fluor 488 conjugate	poly.	goat	ThermoFisher	A11001	1/200

Table 4 *In vitro* knockdown activity of KNTC2 siRNAs. Knockdown activities of KNTC2 siRNAs were evaluated using human and mouse hepatocelluar carcinoma cell lines, Hep3B-luc and Hepa-1c1c7. IC_{50} values of KNTC2 siRNAs were listed separately for human and mouse KNTC2.

	IC_{50} value (pM)	
siRNA	Human (Hep3B-luc)	Mouse (Hepa1c1c7)
KNTC2#1	15	94
KNTC2#2	14	50
KNTC2#3	3	19
KNTC2#4	20	62
KNTC2#5	24	>10,000
KNTC2#6	40	1,454
KNTC2#7	58	>10,000
KNTC2#8	22	>10,000
KNTC2#9	16	455
KNTC2#10	5	>10,000
KNTC2#11	27	>10,000

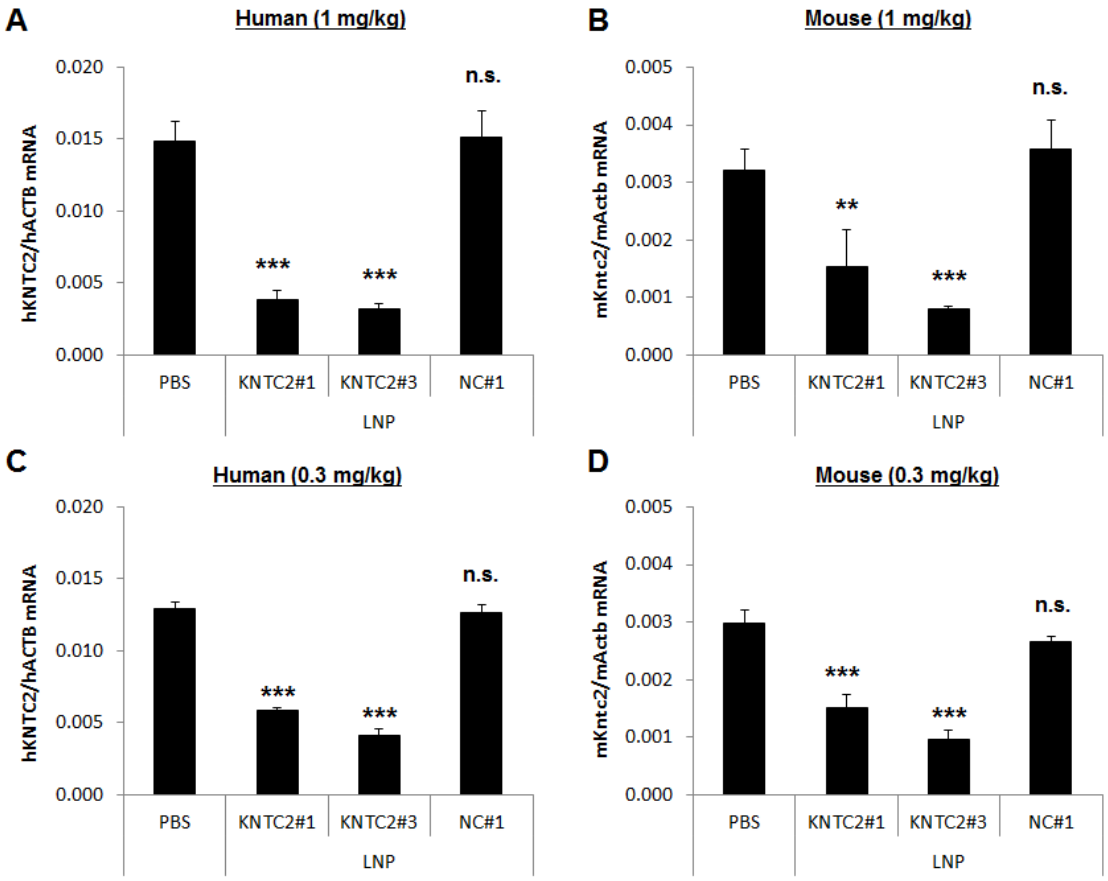

Figure 6 Suppression of human *KNTC2* and mouse *Kntc2* mRNAs by KNTC2 siRNAs in the tumor tissues of HCC model mice. KNTC2 siRNAs (#1 or #3) encapsulated into LNP were intravenously administered to orthotopic HCC model mice of Hep3B-luc cells at the dosage of 1 mg/kg (A, B) or 0.3 mg/kg (C, D). NC#1 was used as a negative control. Knockdown activities were evaluated two days after the single administration. (A, C) Human KNTC2/ACTB mRNA. (B, D) Mouse *Kntc2*/Actb mRNA. Values were represented by mean+SD. n.s., no significant difference; **, $p<0.01$; ***, $p<0.001$ by Dunnett's test (N=3).

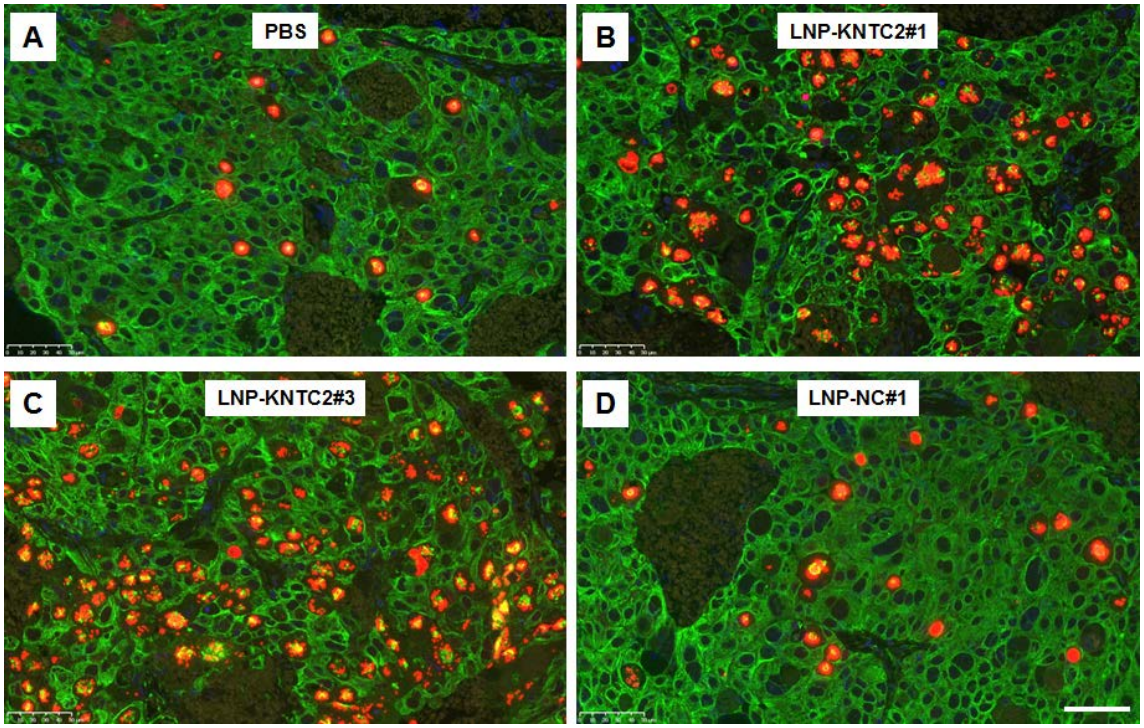

Figure 7 Induction of phosphorylated histone H3 by KNTC2 siRNA in the tumor tissues of HCC model mice. KNTC2 siRNAs (#1 or #3) encapsulated into LNP were intravenously administered to orthotopic HCC model mice of Hep3B-luc cells at the dosage of 1 mg/kg (B, C). NC#1 was used as a negative control (D). Two days after the single administration, orthotopic tumor tissues were dissected to stain phosphorylated histone H3 (red) and alpha-tubulin (green). Scale bar = 50 μm

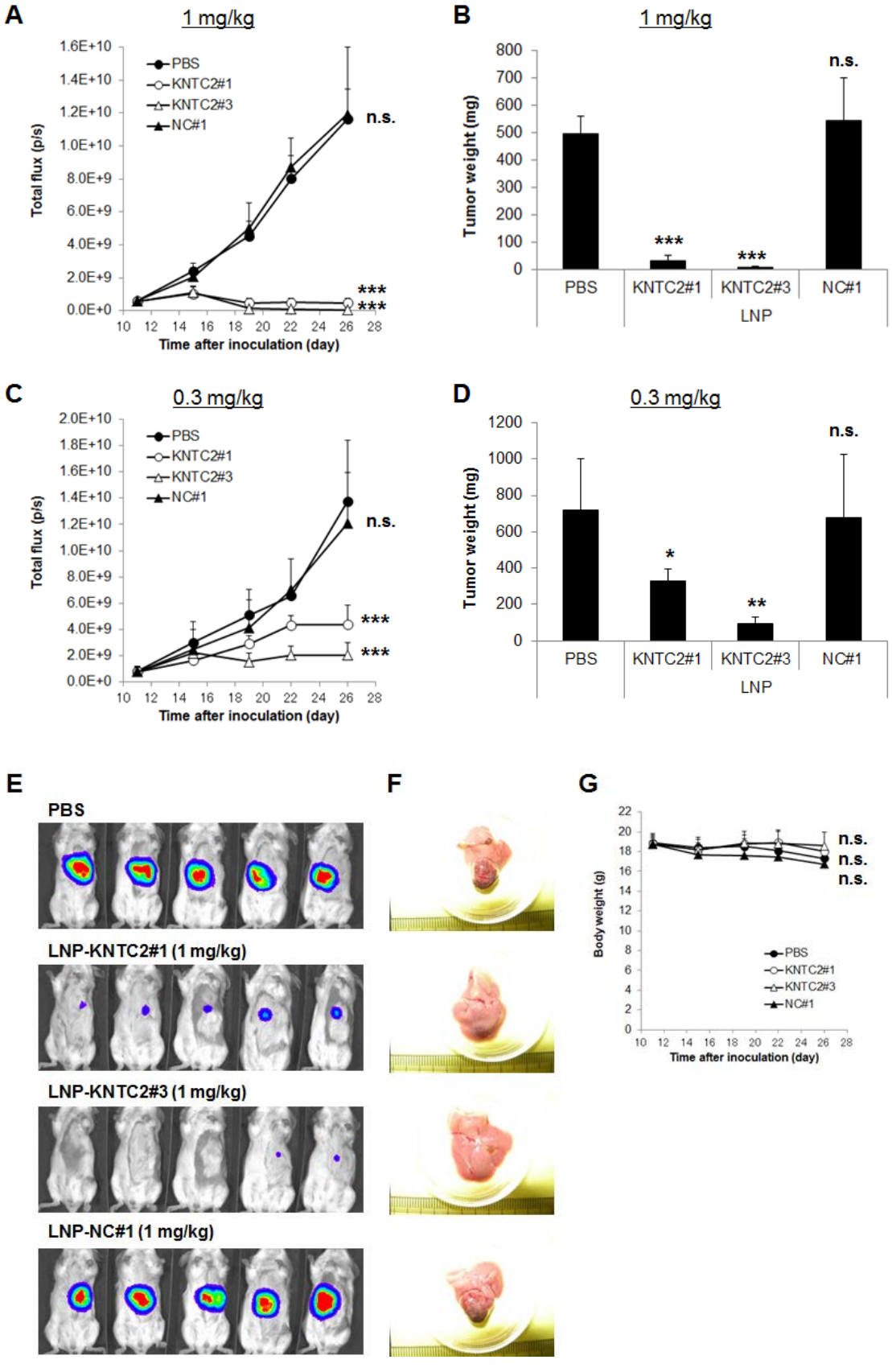
A
1 mg/kg
Total flux (p/s)
Time after inoculation (day)
PBS
KNTC2#1
KNTC2#3
NC#1
n.s.
***
***
B
1 mg/kg
Tumor weight (mg)
n.s.
***
***
PBS
KNTC2#1
KNTC2#3
NC#1
LNP
C
0.3 mg/kg
Total flux (p/s)
Time after inoculation (day)
n.s.
***
***
D
0.3 mg/kg
Tumor weight (mg)
n.s.
*
**
PBS
KNTC2#1
KNTC2#3
NC#1
LNP
E
PBS
LNP-KNTC2#1 (1 mg/kg)
LNP-KNTC2#3 (1 mg/kg)
LNP-NC#1 (1 mg/kg)
F
G
Body weight (g)
Time after inoculation (day)
n.s.
n.s.
n.s.
PBS
KNTC2#1
KNTC2#3
NC#1

Figure 8 Anti-tumor activities of KNTC2 siRNA-LNPs in orthotopic tumor model mice of HCC. KNTC2 siRNAs (KNTC2#1 or KNTC2#3) encapsulated into LNP were repeatedly (twice a week) administered to orthotopic HCC model mice of Hep3B-luc cells at the dosage of 1 mg/kg (A, B, E, F and G) or 0.3 mg/kg (C, D). NC#1 was used as a negative control. Growth inhibitory activities were evaluated by IVIS (A, C, E) and tumor weight (B, D). Tumor tissues were dissected at the end of evaluation (F). Body weights of mice were measured twice a week (G). Values were represented by mean+SD. n.s., no significant difference; *, $p<0.05$; **, $p<0.01$; ***, $p<0.001$ by Dunnett's test (N=5).

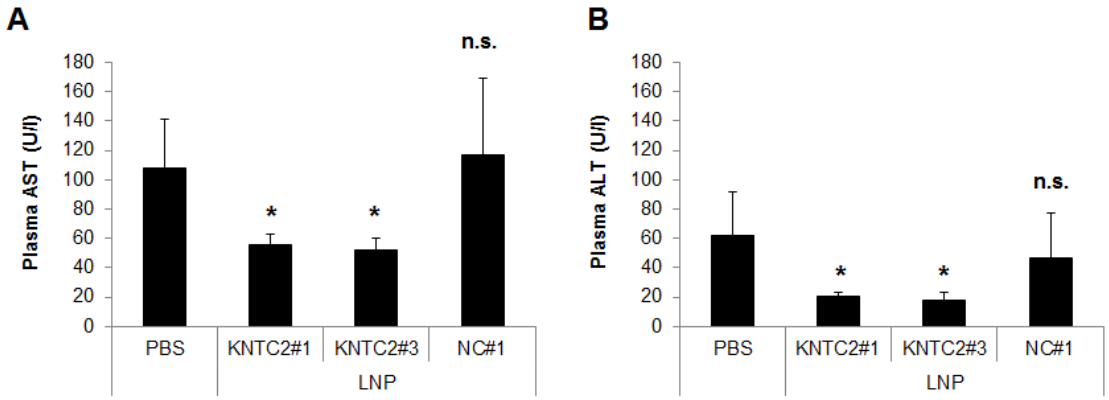

Figure 9 Hepatotoxicities of KNTC2 siRNA-LNPs in orthotopic tumor model mice of HCC. KNTC2 siRNAs (KNTC2#1 or KNTC2#3) encapsulated into LNP were repeatedly (twice a week) administered to orthotopic HCC model mice of Hep3B-luc cells at the dosage of 1 mg/kg. NC#1 was used as a negative control. Plasma AST level (A) and ALT level (B) were measured four days after the fourth administration. Values were represented by mean+SD. n.s., no significant difference; *, $p<0.05$ by Dunnett's test (N=5)

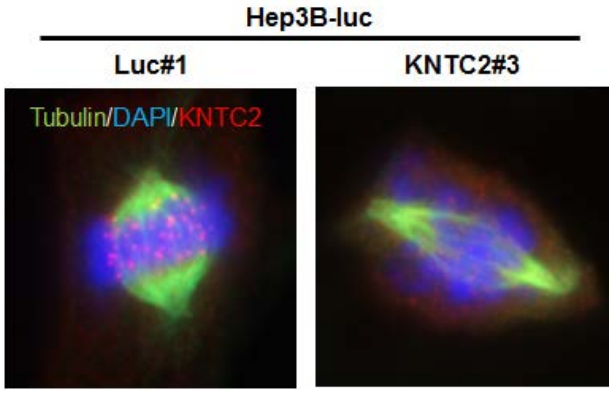

Figure 10 Effect of KNTC2 siRNA on the chromosome alignment in a HCC cell line. Hep3B-luc cells (1×10^5 cells) were seeded in 6 well-plates and cultured overnight. These cells were transfected with KNTC2 siRNA (KNTC2#3) at the concentration of 10 nM using DharmaFECT1 and fixed with formalin 24 hours after the transfection. Luc#1 was used as a negative control. Tubulin (green), DAPI (blue) and KNTC2 (red) were stained and observed using fluorescence microscope.

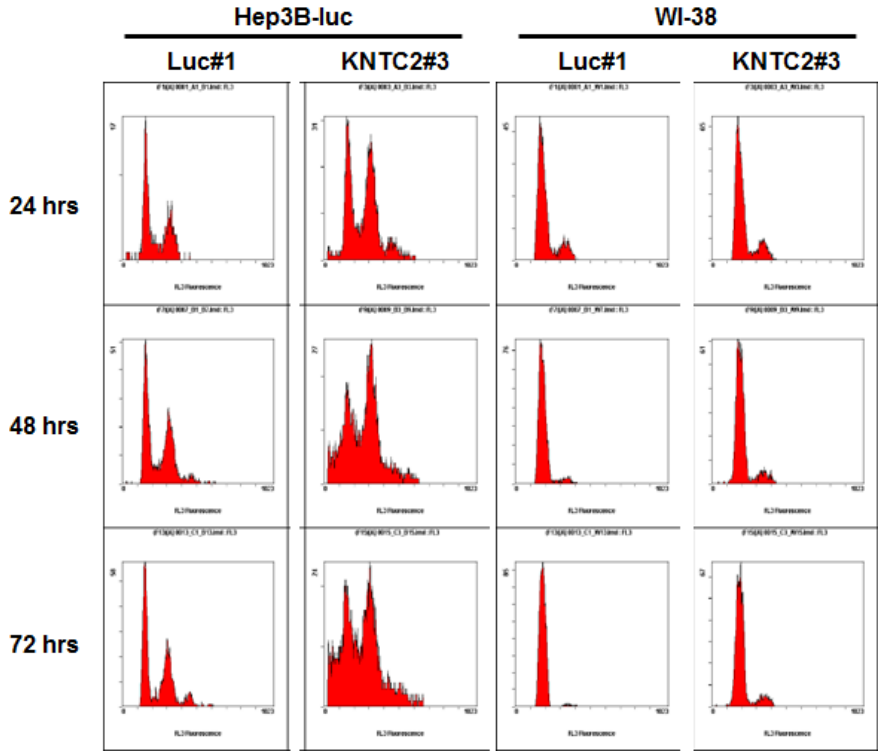

Figure 11 Effect of KNTC2 siRNA on the cell cycles of HCC and normal cell lines. Hep3B-luc cells or WI-38 cells (1×10^5 cells) were seeded in 6 well-plates and cultured overnight. These cells were transfected with KNTC2 siRNA (KNTC2#3) at the concentration of 10 nM using DharmaFECT1. Luc#1 was used as a negative control. Cells were collected using trypsin and fixed with ethanol 24, 48 and 72 hours after the transfection. Nuclear DNAs were stained with propidium iodide and analyzed by Cell Lab Quanta MPL.

Chapter 2 : Anti-tumor activity of KNTC2 siRNA-LNP against lung cancer patient- derived tumor xenografts

Abstract

Using the KNTC2 siRNA-LNP validated in chapter 1, I next evaluated its anti-tumor activities against lung cancer patient-derived tumor xenografts (PDXs) that had been reported to be more relavant to the tumor tissues of cancer patients compared with conventional cancer cell lines. In this chapter, I firstly established three-dimensional (3D) culture systems of lung cancer PDXs (LC-45 and LC-60) and confirmed their correlation with *in vivo* subcutaneous tumor models by checking their sensitivities to an approved drug, erlotinib. Knockdown and anti-tumor activities of KNTC2 siRNA-LNP were clarified in the 3D-culture system and subcutaneous tumor model of LC-60 that was resistant to erlotinib. KNTC2 siRNA-LNP also exhibited *in vivo* knockdown and antitumor activity against LC-45 that was sensitive to erlotinib. These results suggest that KNTC2 siRNA-LNP could be widely applied to lung cancer patients.

Introduction

Tumor tissues are highly heterogeneous. Several types of cell interact with each other making it difficult to predict their drug sensitivities[52]. Reconstruction of this heterogeneity in a preclinical study may provide a method to predict the efficacy of novel anticancer drugs in clinical study[53]. Patient-derived tumor xenografts (PDXs) are established by maintaining the tumor tissues derived from patients with cancer in the flank of immuno-deficient mice[54,55]. Compared with conventional cancer cell lines, PDXs have been reported to be more relevant to the original tumor tissues of patients with cancer in terms of drug sensitivity, heterogeneity and genetic status[56-60]. Accordingly, PDXs may be used for the evaluation of new anticancer drugs[61].

Lung cancer is categorized into small cell lung cancer (SCLC) and non-small cell lung cancer (NSCLC). The most common types of NSCLC are squamous cell carcinoma, adenocarcinoma and large cell carcinoma[62]. These types of NSCLC are further classified into several stages according to their disease status[63]. Several anticancer drugs have been developed for each type of lung cancer. Their molecular targets include epidermal growth factor receptor (EGFR) tyrosine kinase (erlotinib[64], gefitinib[65] and afatinib[66]), rearranged anaplastic lymphoma kinase (crizotinib[67], ceritinib[68] and alectinib[69]), folate-dependent enzymes (pemetrexed[70]), vascular endothelial growth factor (bevacizumab[71]), C-X-C chemokine receptor type 4 (LY2510924[72]) and programmed cell death protein 1 (nivolumab[73]). Although these drugs demonstrated therapeutic effects on several types of lung cancer, other treatment options are desired to increase their combined effects.

In chapter 1, I clarified the tumor-selective *in vivo* growth inhibitory activities of KNTC2 siRNA-LNPs in orthotopic tumor model mice of HCC[74]. However, it remains unclear whether KNTC2 siRNA-LNPs exhibit anti-tumor activities against lung cancer PDXs.

To expand the application of KNTC2 siRNA-LNP to lung cancer PDXs, I investigated its anti-tumor activities in three-dimensional culture system and subcutaneous tumor models of lung cancer PDXs, LC-45 (sensitive to erlotinib) and LC-60 (resistant to erlotinib).

Materials and Methods

Lung cancer PDXs

Lung cancer PDXs, LC-45 (adenocarcinoma) and LC-60 (small or large cell carcinoma) were purchased from the Central Institute for Experimental Animals (Kanagawa, Japan). PDXs were maintained in the flank of BALB/c nude mice (20-25 g; 7-8 weeks old; female; Charles River Laboratories International, Inc., Kanagawa, Japan). When PDXs grew to approximately 1,000 mm^3, PDXs were excised and cryopreserved in small pieces (40-70 μm) using Cell Banker 2 (Nippon Zenyaku Kogyo, Co., Ltd., Fukushima, Japan). Humane endpoint was determined by 20% weight loss and the maximum tumor size was 1,000 mm^3. Mice were maintained in specific pathogen-free conditions with free access to food and water, under a constant temperature of 22±2˚C and a 12/12 h light/dark cycle. All experiments were approved by the Institutional Animal Care and Use Committee in Takeda Pharmaceutical Company Limited (Fujisawa, Japan; approval number 11387).

Chemical modification of siRNAs

KNTC2 siRNA and Luc siRNA (negative control) [15] were synthesized by GeneDesign (Osaka, Japan) and chemically modified with 2'-*O*-methyl ribonucleotide to prevent immune responses, as described previously [45]. Different from chapter 1, phosphorothioate (PS) modifications were not used for KNTC2 siRNA to prevent optical isomers. The sequences and chemical modifications are listed in Table 5.

Encapsulation of siRNAs into lipid nanoparticles

KNTC2 siRNA and Luc siRNA were encapsulated into lipid nanoparticles in the same way as described in chapter 1.

Evaluation of knockdown activities in subcutaneous tumor models of PDXs

Small pieces (~100 mm^3) of PDXs were inoculated in the flank of BALB/c nude mice using a trocar needle (KN-391; Natsume Seisakusho, Co., Ltd., Tokyo, Japan). Tumor sizes were measured with calipers and defined as (major axis) x $(\text{minor axis})^2$ / 2, as previously described. When the tumor sizes reached between 100 and 400 mm^3, 9 mice were selected from a total of 20 mice and divided into three groups (PBS, KNTC2 and Luc) using EXSUS 2014 software (version8.0, CAC Exicare Corporation, Tokyo, Japan). KNTC2 siRNA encapsulated into LNP (KNTC2-LNP) was intravenously administered at 5 mg/kg (n=3). Luc siRNA-LNP was used as the negative control. PBS was administered to the vehicle control group. Knockdown activity was measured 3 days after the single administration. Total RNA was extracted from tumor tissue using TRIzol® (Life Technologies; Thermo Fisher Scientific, Inc.) and reverse transcribed (thermocycling conditions: 25˚C for 10 min; 42˚C for 1 h; and 85˚C for 5 min) using SuperScript VILO cDNA Synthesis kit (Thermo Fisher Scientific, Inc.). The copy numbers of human *KNTC2*, human β-actin (*ACTB*), mouse *Kntc2* and mouse *Actb* mRNA were individually measured by quantitative polymerase chain reaction (using a Real-Time PCR System (Thermo Fisher Scientific, Inc.). Species-specific qPCR primers and probes (Thermo Fisher Scientific, Inc.) are listed in Table 6. Copy numbers of *KNTC2* or *Kntc2* mRNA were individually normalized to *ACTB* or *Actb* mRNA.

Evaluation of growth inhibitory activities in subcutaneous tumor models of PDXs

A total of 10 or 15 mice were selected from 20 or 45 mice (total number of mice, 65), respectively, and divided into two (control and erlotinib) or three (control, KNTC2 and Luc) groups using EXSUS 2014 software. Erlotinib (Carbosynth, Ltd., Compton, UK) was orally administered at 100 mg/kg once a day for 11 days (LC-45) or 5 days (LC-60) In addition, 0.5% methylcellulose was used as the control (n=5). KNTC2-LNP was intravenously administered at 5 mg/kg at three time points, with three days between each administration. Luc siRNA-LNP was used as the negative control. PBS was administered to the vehicle control group. Tumor sizes were measured as aforementioned. Growth inhibitory rate (%) was calculated using the formula: (1- tumor growth of treated group / tumor growth of untreated group) x100%.

Cryopreservation of PDXs for 3D culture systems

PDXs were excised from BALB/c nude mice and cut into small pieces (~100 mm^3). These pieces were digested in Dulbecco's modified eagle's medium (DMEM) high glucose (Thermo Fisher Scientific, Inc.) containing 75 U/ml collagenase type XI (Sigma Aldrich; Merck KGaA, Darmstadt, Germany), 125 μg/ml dispase type II (Thermo Fisher Scientific, Inc.), 2.5% (v/v) fetal bovine serum (Thermo Fisher Scientific, Inc.) and 100 U/ml penicillin/streptomycin at 37˚C. Digestion was terminated prior to complete dispersion of the PDXs. PDXs of intermediate size (between 40 and 100 μm) were collected using a cell strainer and cryopreserved in a Cell Banker 2 (Nippon Zenyaku Kogyo, Co., Ltd.) at -160˚C.

3D-culture of cryopreserved PDXs

Cryopreserved PDXs were suspended in Advanced DMEM/F12 (ratio, 1:1; Thermo Fisher Scientific, Inc.) containing 10 mM 4-(2-hydroxyethyl)-1- piperazine ethanesulfonic acid, 2 mM GlutaMAX-1 (Thermo Fisher Scientific, Inc.), N2 supplement (Thermo Fisher Scientific, Inc.), B27 supplement (Thermo Fisher Scientific, Inc.), 100 U/ml penicillin/streptomycin, 1 mM N-acetylcysteine, 500 nM A-83-01 and 1 μM SB202190 as previously described [75]. Subsequently, PDXs were seeded in U-bottom 96-well plate (Sumitomo Bakelite Co., Ltd., Tokyo, Japan) and cultured in a 5% CO_2-humidified chamber at 37˚C. Growth of PDX was monitored using Cellavista and Cellavista Control and Evaluation Software version 2.1.0.876 (Synentec GmbH, Elmshorn, Germany). Data was omitted when the shape of PDX was not recognized by Cellavista.

Evaluation of knockdown activities in 3D-culture system of PDXs

PDXs were cultured for four days as aforementioned. KNTC2-LNP was added at concentrations of 10 nM, 100 nM and 1 μM (n=6). PDXs were subsequently cultured for an additional three days and mixed together due to each tumor volume being too small to obtain a sufficient amount of total RNA for evaluating knockdown activities. Total RNA was extracted using RNeasy kit (Qiagen GmbH, Hilden, Germany) and reverse-transcribed using SuperScript VILO cDNA Synthesis kit, according to manufacturer's protocols. Knockdown activities were calculated as aforementioned.

Evaluation of growth inhibitory activities in a 3D-culture system of PDXs

PDXs were cultured for three (LC-60) or four (LC-45) days as aforementioned (n=6). KNTC2-LNP was added at concentrations ranging from 10 nM, 100 nM and 1 μM. Erlotinib (Carbosynth) was added at concentrations of 10 nM, 100 nM, 1 μM and 10 μM using a sample-dispensing machine (HP D300 Digital Dispenser, Tecan Japan Co., Ltd., Kawasaki, Japan). Growth inhibitory rate was calculated using the formula as aforementioned.

Statistical analysis

Data was statistically analyzed using EXSUS 2014 software. Significance among groups was analyzed using Bartlett's test followed by Dunnett's test (in vivo studies) or Williams' test (in vitro studies). $P<0.05$ was considered to indicate a statistically significant difference.

Results

Sensitivities of lung cancer PDXs to erlotinib *in vitro* and *in vivo*

To select different types of lung cancer PDXs for the evaluation of KNTC2-LNP, the sensitivities of several PDXs to erlotinib (an approved drug for patients with lung cancer) were investigated. Among those PDXs, LC-45 exhibited relatively high sensitivity to erlotinib in a subcutaneous tumor model (Fig. 12A). Repeated oral administration of erlotinib (100 mg/kg, once a day) significantly ($P<0.001$) inhibited the tumor growth of LC-45 by 86%. In contrast, the same dosage of erlotinib did not inhibit the tumor growth of LC-60 (Fig. 12B).

Sensitivities of LC-45 and LC-60 to erlotinib were also investigated in 3D-culture systems. Erlotinib significantly ($P<0.001$) inhibited the growth of LC-45 by 81% at the concentration of 1 μM (Fig. 13A). The growth of LC-60 was not inhibited by erlotinib at the same concentration indicating that LC-60 was less sensitive to erlotinib compared with LC-45 (Fig. 13B).

Encapsulation of siRNAs into LNP

The particle sizes of KNTC2 siRNA-LNP and Luc siRNA-LNP were 75 and 73 nm, respectively. PdIs were 0.012 and 0.022. The entrapment efficiencies were 98.2 and 97.6%, demonstrating that each siRNA was successfully encapsulated into LNP.

Knockdown and growth inhibitory activity of KNTC2-LNP in 3D-culture system of LC-60

The knockdown activities of KNTC2-LNP were 60% at 10 nM, 79% at 100 nM and 88% at 1 μM in 3D-culture systems of LC-60 (Fig. 14A). The knockdown activities of Luc siRNA-LNP (negative control) were markedly decreased compared with KNTC2-LNP, indicating the specificity of KNTC2 siRNA (Fig. 14B).

Tumor growth of LC-60 was significantly inhibited by KNTC2-LNP at 100 nM and 1 μM ($P<0.001$; Fig. 15A). The growth inhibition rates were 21 and 63%, respectively. Luc siRNA-LNP (negative control) did not significantly inhibit the growth of LC-60 at the same concentrations, indicating that growth inhibition was specifically caused by the suppression of human KNTC2 mRNA expression (Fig. 15B).

Knockdown and growth inhibitory activities of KNTC2-LNP in subcutaneous tumor model mice of lung cancer PDXs

Knockdown and growth inhibitory activities of KNTC2-LNP were further investigated in the subcutaneous tumor model of LC-60. Single intravenous administration of KNTC2-LNP (5 mg/kg) significantly suppressed the expression levels of human KNTC2 and mouse *Kntc2* mRNA in LC-60 by 27% and 46%, respectively ($P<0.01$; Figs. 16A-B). Luc siRNA-LNP (negative control) did not exhibit knockdown activities at the same dosage. Repeated intravenous administration of KNTC2-LNP (5 mg/kg, twice a week) significantly inhibited the growth of LC-60 by 67% ($P<0.001$; Fig. 16C). Luc siRNA-LNP did not inhibit the growth of LC-60 indicating that the growth inhibition was specifically caused by the suppression of human KNTC2 and mouse *Kntc2* mRNA expression levels.

Knockdown and growth inhibitory activities of KNTC2-LNP were also investigated using another lung cancer PDX, LC-45. Single intravenous administration of KNTC2-LNP (5 mg/kg) significantly suppressed the expression levels of human KNTC2 and mouse *Kntc2* mRNA in LC-45 by 63 and 60%, respectively ($P<0.001$; Figs. 17A-B). Repeated intravenous administration of KNTC2-LNP (5 mg/kg, twice a week) significantly inhibited the growth of LC-45 by 63% ($P<0.01$; Fig. 17C) suggesting that KNTC2-LNP exhibits antitumor activity against various types of lung cancer PDXs.

Discussion

To expand the application of KNTC2 siRNA-LNP, I evaluated its anti-tumor activities in 3D-culture systems and subcutaneous tumor models of lung cancer PDXs, LC-45 and LC-60.

Lung cancer PDXs implanted into the flank of immuno-deficient mice were estimated to be composed of lung cancer patient-derived human cells and host mouse-derived stromal cells[76]. Stromal cells have been reported to affect the proliferation of cancer cells in tumor tissues[77]. Therefore, in the present study, KNTC2 siRNA that suppressed not only human *KNTC2* mRNA but also mouse *Kntc2* mRNA was selected in order to clarify the involvement of KNTC2 in human-derived cancer cells and mouse-derived stromal cells (Figs. 16-17). The knockdown activities of KNTC2 siRNA were sufficient to inhibit the *in vivo* growth of LC-60 and LC-45. Negative control Luc siRNA did not inhibit the growth of these PDXs, indicating that their growths were dependent on KNTC2.

Notably, KNTC2 siRNA inhibited the growth of LC-60 that was resistant to an approved drug, erlotinib (Figs. 15-16). According to previous studies, KNTC2 siRNA was estimated to impair the chromosome segregation of LC-60 leading to cell cycle arrest and apoptosis[78,79]. This molecular mechanism is distinct from that of erlotinib, which inhibits the auto-phosphorylation of EGFR tyrosine kinase[80]. Inhibitors of EGFR tyrosine kinase were reported to be ineffective in patients with lung cancer with mutations in *KRAS*[81] or *EGFR*[82]. LC-60 exhibited a mutated *KRAS* gene (G12V). Therefore, KNTC2 may be a therapeutic target for patients with lung cancer that is resistant to erlotinib.

Several types of 3D-culture systems have been developed for PDXs to increase the efficiency of drug screening[83-85]. Efficiency of evaluating KNTC2 siRNA was increased by establishing 3D-culture systems of LC-45 and LC-60. In the case of erlotinib, the results of 3D-culture systems were similar to that of subcutaneous tumor models (Figs. 12-13). These results were consistent with previous reports demonstrating the similarities of 3D-culture systems to subcutaneous tumor models using other lung cancer PDXs [86,87].

The maximum knockdown activity of KNTC2-LNP in the 3D-culture system was sufficient to inhibit the growth of LC-60 and predict the result of *in vivo* study (Figs. 14-16). In contrast, growth inhibitory activity of KNTC2-LNP was not detected in the 3D-culture system of LC-45 (data not shown). The reason for these results was speculated to be that the maximum knockdown activity of KNTC2-LNP was insufficient to inhibit the growth of LC-45. Applicability of the 3D-culture system to the evaluation of KNTC2-LNP was considered to be different between PDXs.

In conclusion, I established *in vitro* 3D-culture systems of lung cancer PDXs and confirmed their correlation with *in vivo* subcutaneous tumor model mice. Anti-tumor activities of KNTC2 siRNA-LNP were clarified in the 3D-culture system and subcutaneous tumor model of LC-60 that was resistant to erlotinib. KNTC2 siRNA-LNP also inhibited the *in vivo* growth of LC-45 that was sensitive to erlotinib. These results indicated that KNTC2 siRNA-LNP could be widely applied to lung cancer patients.

Tables and Figures

Table 5 List of chemically modified siRNAs for Luc and KNTC2.

siRNA	Strand	Sequence
Luc siRNA	Sense	5'-r(CUUACGCUGAGUACUUCGA)-dTsdT-3'
	Antisense	5'-r(UCGAAGUACUCAGCGUAAG)-dTsdT-3'
KNTC2 siRNA	Sense	5'-r(UAGUCAACUUGGUAUAUUU)-dTdT-3'
	Antisense	5'-r(AAAUAUACCAAGUUGACUA)-dTdT-3'

r, ribonucleotide; d, deoxy-ribonucleotide; s, phosphorothioate modification; underline, 2'-*O*-methyl ribonucleotide.

Table 6 List of quantitative PCR primers and probes specific for human *KNTC2* and mouse *Kntc2* mRNAs.

Gene	Sequence
Human *KNTC*2	
Forward primer	5'-d(GAGGTACATAAACTTGAGCCCTGTATT)-3'
Reverse primer	5'-d(TGCTGAGAATTCCAAAGGTTATGA)-3'
Probe	5'-d(TGGCACCAGCCTCGGGATTAAACTTAA)-3'
Human *ACTB*	
Forward primer	5'-d(CCTGGCACCCAGCACAAT)-3'
Reverse primer	5'-d(GCCGATCCACACGGAGTACT)-3'
Probe	5'-d(ATCAAGATCATTGCTCCTCCTGAGCGC)-3'
Mouse *Kntc2*	
Forward primer	5'-d(GAATAAAAAGAGGCATCTGGAGGATAC)-3'
Reverse primer	5'-d(CCTCCTTCAGCATCCTCACAGT)-3'
Probe	5'-d(CAACTGAACACCATGAAAACGGAAAGCAA)-3'
Mouse *Actb*	
Forward primer	5'-d(CACTATTGGCAACGAGCGG)-3'
Reverse primer	5'-d(TCCATACCCAAGAAGGAAGGC)-3'
Probe	5'-d(TCCGATGCCCTGAGGCTCTTTTCC)-3'

d, deoxy-ribonucleotide; KNTC2, kinetochore-associated protein 2; ACTB, β-actin.

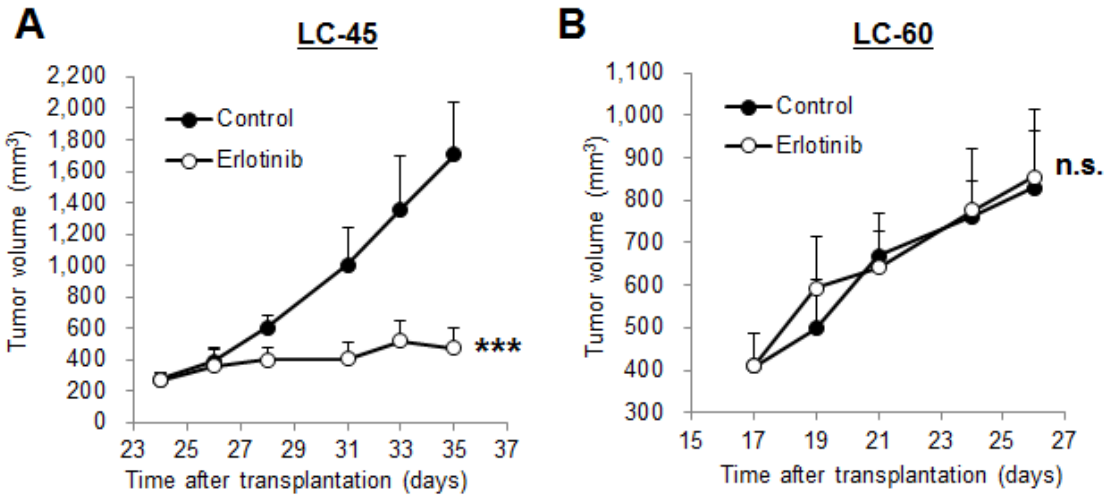

Figure 12 Sensitivities of lung cancer patient-derived tumor xenografts to erlotinib in subcutaneous tumor model mice. LC-45 (A) and LC-60 (B) were inoculated in the flank of BALB/c nude mice. Erlotinib (100 mg/kg) was orally administered once a day during the test periods. Control group mice were treated with 0.5% methylcellulose. Values are presented as the mean+SD (n=5). n.s., no significance; ***, P<0.001 by Dunnett's test.

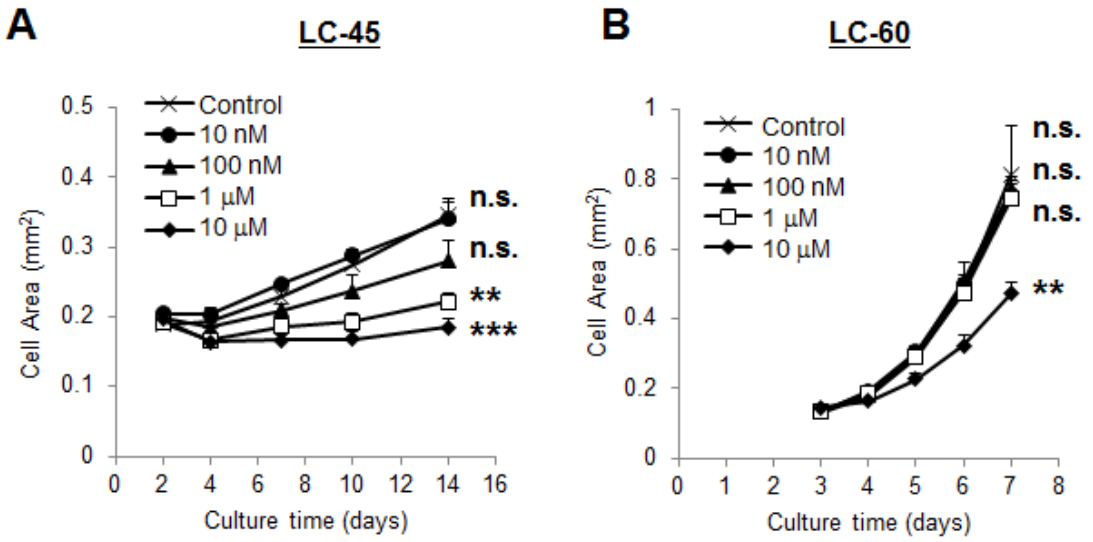

Figure 13 Sensitivities of lung cancer patient-derived tumor xenografts to erlotinib in 3D-culture systems. Growth inhibitory activities of erlotinib were evaluated in 3D-culture systems of (A) LC-45 and (B) LC-60. The concentrations of erlotinib were 10, 100 nM, 1 and 10 μM. Values are presented as the mean+SEM (n=4). n.s., no significance; **, P<0.005; ***, P<0.0005 compared with control by Williams' test.

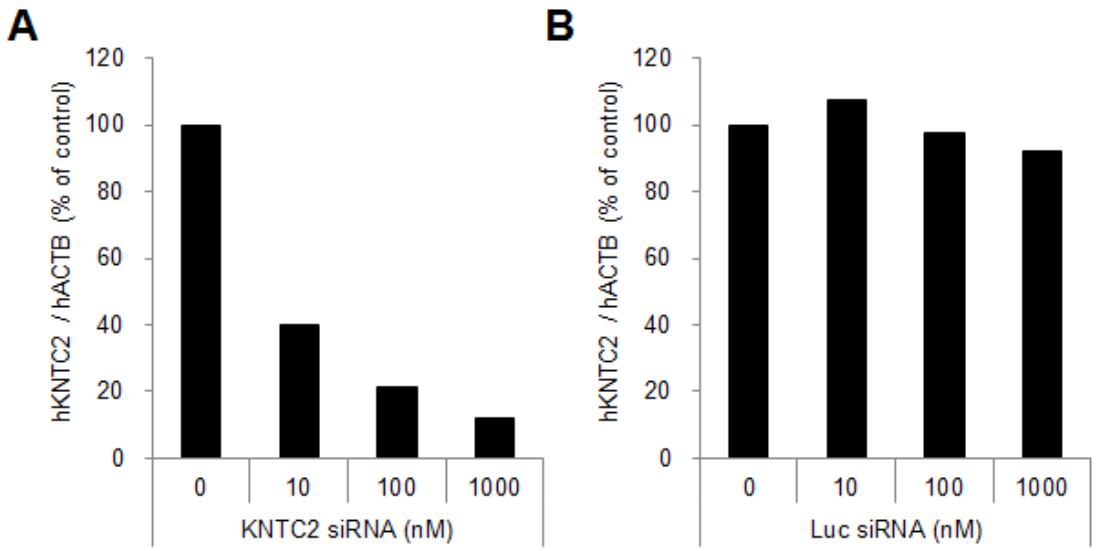

Figure 14 Knockdown activities of KNTC2-LNP in 3D-culture system of LC-60. The knockdown activity of KNTC2-LNP (10 nM - 1 μM) was evaluated in a 3D-culture system of LC-60 (A). Luc siRNA-LNP was used as a negative control (B). The expression levels of human KNTC2 mRNAs were measured three days after the addition of lipid nanoparticles (n=6).

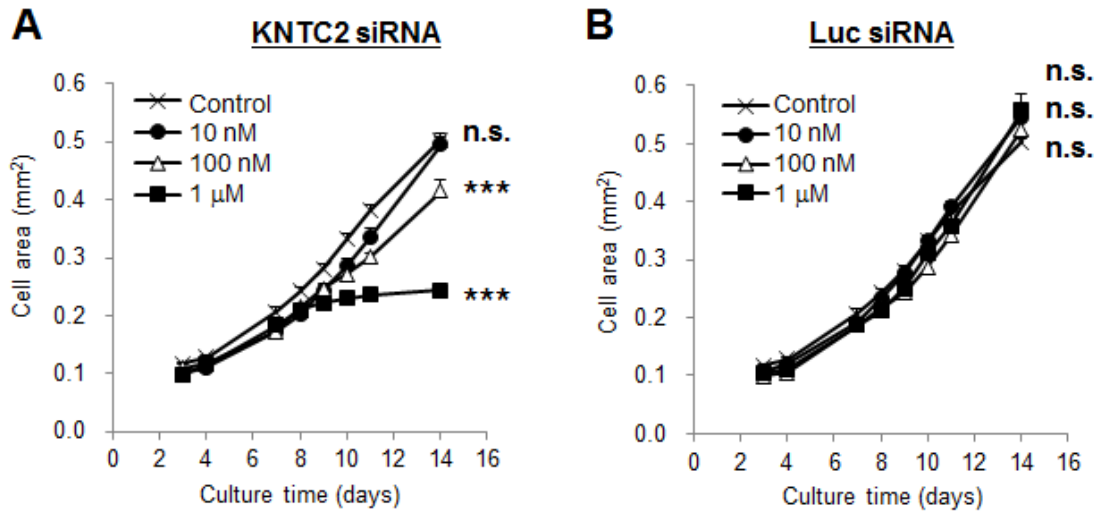

Figure 15 Growth inhibitory activity of KNTC2-LNP in 3D-culture system of LC-60. Growth inhibitory activity of KNTC2-LNP (A) was evaluated in 3D-culture systems of LC-60. Luc siRNA-LNP (B) was used as a negative control. These siRNAs were evaluated at 10, 100 nM and 1 μM. Values are presented as the mean+SEM (n=5 or 6). n.s., no significance; ***, P<0.0005 compared with control by Williams' test.

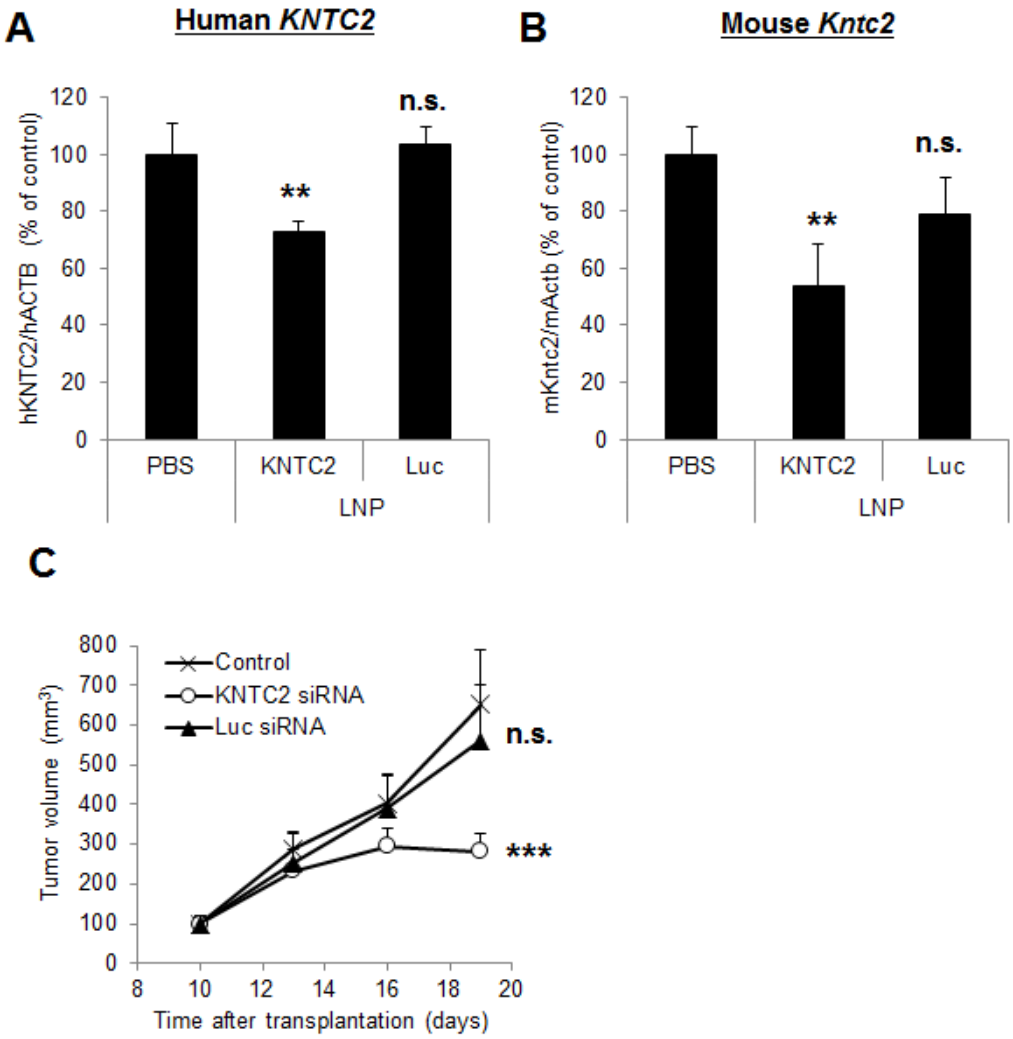

Figure 16 Knockdown and growth inhibitory activities of KNTC2-LNP in subcutaneous tumor model mice of LC-60. Knockdown activities of KNTC2-LNP (5 mg/kg) were evaluated three days following a single intravenous administration. PBS and Luc siRNA-LNP were used as controls. The expression levels of human KNTC2 mRNA (A) and mouse *Kntc2* mRNA (B) were investigated. Values are presented as the mean+SD (n=3). (C) Growth inhibitory activities of KNTC2-LNP (5 mg/kg) were evaluated during repeated intravenous administration (twice a week). Values are presented as the mean+SD (n=5). n.s., no significance; **, $P<0.01$; ***, $P<0.001$ compared with PBS/control by Dunnett's test.

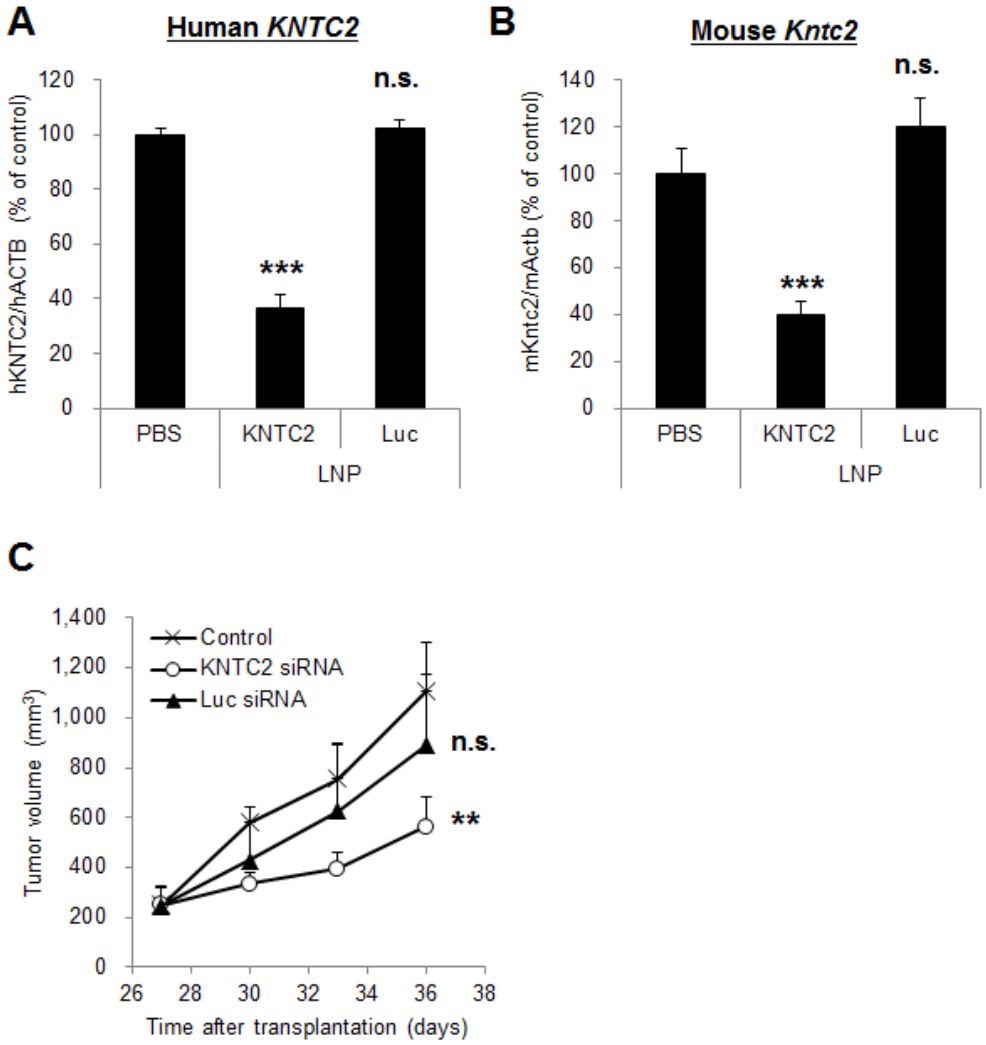

Figure 17 Knockdown and growth inhibitory activities of KNTC2-LNP in subcutaneous tumor model mice of LC-45. Knockdown activities of KNTC2-LNP (5 mg/kg) were evaluated three days following a single intravenous administration. PBS and Luc siRNA-LNP were used as controls. The expression levels of human KNTC2 mRNA (A) and mouse *Kntc2* mRNA (B) were investigated. Values are presented as the mean+SD (n=3). (C) Growth inhibitory activities of KNTC2-LNP (5 mg/kg) were evaluated during repeated intravenous administration (twice a week). Values are presented as the mean+SD (n=5). n.s., no significance; **, $P<0.01$; ***, $P<0.001$ compared with PBS/control by Dunnett's test.

General Discussion

To clarify the involvement of KNTC2 in the growth of tumor tisses and show the possibility of developing KNTC2 siRNA drug for cancer therapy, I firstly selected highly potent siRNAs targeting KNTC2 *in vitro* and encapsulated them into a LNP for *in vivo* studies. Anti-tumor activities of KNTC2 siRNA-LNPs were confirmed in orthotopic tumor model mice of HCC (chapter 1) and subcutaneous tumor model mice of lung cancer PDX (chapter 2).

Tumor tissues of cancer patients are rich in diversity and highly heterogenous. It is generally difficult to predict efficacies of anti-cancer drugs and determine the optimal dosage for each type of cancer patient. Therefore it was important to confirm the anti-tumor activities of KNTC2 siRNAs in several types of tumor models (HCC and lung cancer PDXs). The administration dosages of KNTC2 siRNA required to show anti-tumor activities were different between HCC model (0.3 mg/kg) and PDX models (5 mg/kg) probably because the efficiencies of deliverying KNTC2 siRNAs were different between these models. The *in vivo* knockdown efficiencies of KNTC2 siRNA were lower in PDX models compared with HCC model (Figs. 6, 16-17). According to a third-party report on a phase I clinical trial of siRNA-LNP, it seemed to be difficult to predict their knockdown efficiencies in cancer patients[22]. Predictive biomarkers were desired to estimate the knockdown efficiencies for each tumor type. 3D-culture systems of PDX as mentioned in chapter 2 might be one of the solutions to predict the compatibility of each cancer patient and siRNA-LNP.

Liver is the most accessible tissue for siRNA-LNP. The first approved siRNA drug was designed to target transthyretin gene in the liver of patients with hereditary

transthyretin amyloidosis[88]. Among a wide variety of cancer models, HCC model seemed to be most suitable for the evaluation of siRNA-LNP[21]. Therefore I firstly selected orthotopic tumor model mice of HCC to evaluate the tumor selectivity of KNTC2 siRNA (Chapter 1). Using siRNAs that are common in human KNTC2 and mouse *Kntc2*, I could simultaneously evaluate the anti-tumor activities and hepatotoxicity in tumor tissues of HCC mixed with normal hepatocytes. The results indicated that anti-tumor activities of KNTC2 siRNAs were tumor selective (Fig. 8-9).

To expand the application of KNTC2 siRNA-LNP, I next confirmed its anti-tumor activity in lung cancer PDX models that were reported to be more relevant to cancer patients (Chapter 2). This was the first report on the relationship between KNTC2 and PDX although there had been some reports on KNTC2 and commercially available cancer cell lines. My study indicated that KNTC2 siRNA-LNP could be applied to lung cancer patients who are resistant to an approved drug, erlotinib (Figs. 12, 16). It is important for cancer patient to be suggested as much options as posssible because the heterogeneity of tumor tissues makes it difficult to develop anti-cancer drugs that were widely effective.

Other groups have developed small molecules targeting KNTC2 and demonstrated their *in vivo* anti-tumor activities. These small molecules, such as INH1[78], TAI-1[89], TAI-95[44] and TH-39[90], were designed to inhibit the interaction between KNTC2 and a mitotic kinase, NIMA-related kinase 2 (Nek2) because phosphorylation of Ser165 in KNTC2 by Nek2 is critical for the modulation of chromosome segregation[91]. Cytotoxicities of TAI-1 and TAI-95 were checked *in vitro* using normal human fibloblast cell line, WI-38. Furthermore, hepatotoxicity and renal toxicity of TAI-1 were checked *in vivo* using CB17 SCID mice. However, its therapeutic window

was not clear because the dosage regimen of TAI-1 was slightly different between tumor xenograft models and toxicological studies. Developments of TAI-1 and its derivatives are not progressing by unknown reason. It is generally difiicult to control the specificity of small molecules. In contrast, the specificity of siRNA is generally high when used in low doses. I could confirm the anti-tumor acitivities of KNTC2 siRNA at the dosage of 5 mg/kg in PDX models (Figs. 16-17). It might be possible to show the superiority of siRNA over small molecules in terms of specificity at therapeutic dosages.

The mechanism of action is different between KNTC2 siRNA and small molecules targeting KNTC2 protein. As mentioned above, small molecules intercept the protein-protein interaction between KNTC2 and Nek2. They do not decrease the expression level of KNTC2 protein. In contrast, KNTC2 siRNA degrades KNTC2 mRNA and decreases KNTC2 protein. There must be some biological differences such as downstream signaling, compensation of decreased KNTC2 by other protein or acquisition of drug resistance. I clarified that the phosphorylation of histone H3 (p-HH3) is a pharmacodynamic marker of KNTC2 siRNA (Fig. 7). There is no report that demonstrated p-HH3 by small molecules targeting KNTC2. This marker is desired to be validated in clinical trials.

In addition to KNTC2, there are many other molecules that play important role in chromosome segregation (Fig. 2). Some of these molecules are candidate targets for cancer therapy. For examples, there is a report that demonstrated *in vivo* anti-tumor activity of NUF2 shRNA using lentiviral vector and human pancreatic cancer cell line[92]. Another report demonstrated *in vitro* anti-tumor activitiy of Spc25 shRNA using lentiviral vector and human prostate cancer cell line[93]. Small molecules have also been developed targeting aurora kinases, CDK1, PLK1, EG5 CENP-E and 26S proteasome

complex[94]. Some of them were effective in clinical trials but most of their effects were low when used in single agent probably because tumor tissues acquire resistance. Severe adverse events such as neuropathies were also concerned. Considering the situation, KNTC2 seemed to be an ideal drug target because its expression profile was highly specific to tumor tissues of cancer patients. In addition, KNTC2 siRNA could be used in combination with pre-existing drugs because their mechanism of actions are different from that of KNTC2 siRNA.

In conclusion, I clarified the tumor-selective *in vivo* growth inhibitory activites of KNTC2 siRNA in orthotopic tumor model mice of hepatocellular carcinoma (Chapter 1)[74] and expanded its application to subcutanenous tumor model mice of lung cancer patient-derived tumor xenografts (Chapter 2)[95]. These results indicated that KNTC2 siRNA could be applied to other types of tumor models. Using the experimental procesure established in this study, candidate target molecules other than KNTC2 would be efficiently evaluated just by exchanging the sequence of siRNA. Therefore this study indicated the possibility of siRNA drugs for many types of cancer patients and target molecules.

Acknowledgements

I am deeply grateful to Associate Professors Kazuichi Sakamoto, Yukihiko Toquenaga, Kentaro Nakano, Professors Chikafumi Chiba and Kazuto Nakada, University of Tsukuba, for guiding my work and valuable discussions through my doctoral program.

I am very thankful to Drs. Keiji Yamamoto, Kazuhiro Ogi, Michiyasu Takeyama, Hirokazu Matsumoto, Toshiyuki Nomura and Yuji Kawamata, Takeda Pharmaceutical Company Limited, for guiding my work and valuable discussions through my work.

I appreciate Dr. Shumpei Murata, Mr Yoshiki Katou, Ms. Kuniko Kikuchi, Dr Hiroshi Uejima, Ms. Mika Teratani, Mr. Yasutaka Hoashi, Mr. Eriya Kenjo, Dr. Satoru Matsumoto, Dr. Masahiro Nogami, Mr. Kentaro Otake, Takeda Pharmaceutical Company Limited, for their contributions and helpful supports.

I also thank Dr. Nobuyuki Miyajima, Dr. Rumiko Ochiai, Dr Tadahiro Nambu, Mr Yuji Baba, Dr Kazuhide Nakamura and Dr Toshiya Tamura,Takeda Pharmaceutical Company Limited, for valuable suggestions and comments.

I also thank Ms.Syu Morita and Ms. Kaori Konno, Takeda Pharmaceutical Company Limited, for their technical support.

Finally, I would like to appreciate my family for supporting my life in the University of Tsukuba.

References

1 Tang, N. H. & Toda, T. MAPping the Ndc80 loop in cancer: A possible link between Ndc80/Hec1 overproduction and cancer formation. *BioEssays : news and reviews in molecular, cellular and developmental biology* **37**, 248-256, doi:10.1002/bies.201400175 (2015).

2 Maiato, H., DeLuca, J., Salmon, E. D. & Earnshaw, W. C. The dynamic kinetochore-microtubule interface. *Journal of cell science* **117**, 5461-5477, doi:10.1242/jcs.01536 (2004).

3 Dhatchinamoorthy, K., Mattingly, M. & Gerton, J. L. Regulation of kinetochore configuration during mitosis. *Current genetics* **64**, 1197-1203, doi:10.1007/s00294-018-0841-9 (2018).

4 Chen, Y., Riley, D. J., Chen, P. L. & Lee, W. H. HEC, a novel nuclear protein rich in leucine heptad repeats specifically involved in mitosis. *Molecular and cellular biology* **17**, 6049-6056 (1997).

5 Kaneko, N. *et al.* siRNA-mediated knockdown against CDCA1 and KNTC2, both frequently overexpressed in colorectal and gastric cancers, suppresses cell proliferation and induces apoptosis. *Biochemical and biophysical research communications* **390**, 1235-1240, doi:10.1016/j.bbrc.2009.10.127 (2009).

6 Qu, Y., Li, J., Cai, Q. & Liu, B. Hec1/Ndc80 is overexpressed in human gastric cancer and regulates cell growth. *Journal of gastroenterology* **49**, 408-418, doi:10.1007/s00535-013-0809-y (2014).

7 Bieche, I. *et al.* Expression analysis of mitotic spindle checkpoint genes in breast carcinoma: role of NDC80/HEC1 in early breast tumorigenicity, and a two-gene signature for aneuploidy. *Molecular cancer* **10**, 23, doi:10.1186/1476-4598-10-23 (2011).

8 Hayama, S. *et al.* Activation of CDCA1-KNTC2, members of centromere protein complex, involved in pulmonary carcinogenesis. *Cancer research* **66**, 10339-10348, doi:10.1158/0008-5472.can-06-2137 (2006).

9 Meng, Q. C. *et al.* Overexpression of NDC80 is correlated with prognosis of pancreatic cancer and regulates cell proliferation. *American journal of cancer research* **5**, 1730-1740 (2015).

10 Wu, S. Y. *et al.* 2'-OMe-phosphorodithioate-modified siRNAs show increased loading into the RISC complex and enhanced anti-tumour activity. *Nature communications* **5**, 3459, doi:10.1038/ncomms4459 (2014).

11 Ferretti, C. *et al.* Expression of the kinetochore protein Hec1 during the cell cycle in normal and cancer cells and its regulation by the pRb pathway. *Cell cycle (Georgetown, Tex.)* **9**, 4174-4182, doi:10.4161/cc.9.20.13457 (2010).

12 Gurzov, E. N. & Izquierdo, M. RNA interference against Hec1 inhibits tumor growth in vivo. *Gene therapy* **13**, 1-7, doi:10.1038/sj.gt.3302595 (2006).

13 Blair, C. D. & Olson, K. E. The role of RNA interference (RNAi) in arbovirus-vector interactions. *Viruses* **7**, 820-843, doi:10.3390/v7020820 (2015).

14 Fire, A. *et al.* Potent and specific genetic interference by double-stranded RNA in Caenorhabditis elegans. *Nature* **391**, 806-811, doi:10.1038/35888 (1998).

15 Elbashir, S. M. *et al.* Duplexes of 21-nucleotide RNAs mediate RNA interference in cultured mammalian cells. *Nature* **411**, 494-498, doi:10.1038/35078107 (2001).

16 Fellmann, C. & Lowe, S. W. Stable RNA interference rules for silencing. *Nature cell biology* **16**, 10-18, doi:10.1038/ncb2895 (2014).

17 Aigner, A. Gene silencing through RNA interference (RNAi) in vivo: strategies based on the direct application of siRNAs. *Journal of biotechnology* **124**, 12-25, doi:10.1016/j.jbiotec.2005.12.003 (2006).

18 Akinc, A. *et al.* Targeted delivery of RNAi therapeutics with endogenous and exogenous ligand-based mechanisms. *Molecular therapy : the journal of the American Society of Gene Therapy* **18**, 1357-1364, doi:10.1038/mt.2010.85 (2010).

19 Miele, E. *et al.* Nanoparticle-based delivery of small interfering RNA: challenges for cancer therapy. *International journal of nanomedicine* **7**, 3637-3657, doi:10.2147/ijn.s23696 (2012).

20 Tam, Y. Y., Chen, S. & Cullis, P. R. Advances in Lipid Nanoparticles for siRNA Delivery. *Pharmaceutics* **5**, 498-507, doi:10.3390/pharmaceutics5030498 (2013).

21 Judge, A. D. *et al.* Confirming the RNAi-mediated mechanism of action of siRNA-based cancer therapeutics in mice. *The Journal of clinical investigation* **119**, 661-673, doi:10.1172/jci37515 (2009).

22 Tabernero, J. *et al.* First-in-humans trial of an RNA interference therapeutic targeting VEGF and KSP in cancer patients with liver involvement. *Cancer discovery* **3**, 406-417, doi:10.1158/2159-8290.cd-12-0429 (2013).

23 Zhang, C. Y., Yuan, W. G., He, P., Lei, J. H. & Wang, C. X. Liver fibrosis and hepatic stellate cells: Etiology, pathological hallmarks and therapeutic targets. *World journal of gastroenterology* **22**, 10512-10522, doi:10.3748/wjg.v22.i48.10512 (2016).

24 Lee, J. M. & Choi, B. I. Hepatocellular nodules in liver cirrhosis: MR evaluation. *Abdominal imaging* **36**, 282-289, doi:10.1007/s00261-011-9692-2 (2011).

25 Mohamad, B. *et al.* Characterization of hepatocellular carcinoma (HCC) in

non-alcoholic fatty liver disease (NAFLD) patients without cirrhosis. *Hepatology international* **10**, 632-639, doi:10.1007/s12072-015-9679-0 (2016).

26 Dutta, R. & Mahato, R. I. Recent advances in hepatocellular carcinoma therapy. *Pharmacology & therapeutics* **173**, 106-117, doi:10.1016/j.pharmthera.2017.02.010 (2017).

27 Aravalli, R. N., Steer, C. J. & Cressman, E. N. Molecular mechanisms of hepatocellular carcinoma. *Hepatology (Baltimore, Md.)* **48**, 2047-2063, doi:10.1002/hep.22580 (2008).

28 Bertino, G. *et al.* Hepatocellular carcinoma: novel molecular targets in carcinogenesis for future therapies. *BioMed research international* **2014**, 203693, doi:10.1155/2014/203693 (2014).

29 Liu, W., Zhou, J. G., Sun, Y., Zhang, L. & Xing, B. C. Hepatic Resection Improved the Long-Term Survival of Patients with BCLC Stage B Hepatocellular Carcinoma in Asia: a Systematic Review and Meta-Analysis. *Journal of gastrointestinal surgery : official journal of the Society for Surgery of the Alimentary Tract* **19**, 1271-1280, doi:10.1007/s11605-015-2811-6 (2015).

30 Xu, D. W., Wan, P. & Xia, Q. Liver transplantation for hepatocellular carcinoma beyond the Milan criteria: A review. *World journal of gastroenterology* **22**, 3325-3334, doi:10.3748/wjg.v22.i12.3325 (2016).

31 Wang, Y. X., De Baere, T., Idee, J. M. & Ballet, S. Transcatheter embolization therapy in liver cancer: an update of clinical evidences. *Chinese journal of cancer research = Chung-kuo yen cheng yen chiu* **27**, 96-121, doi:10.3978/j.issn.1000-9604.2015.03.03 (2015).

32 Yu, J. I. & Park, H. C. Radiotherapy as valid modality for hepatocellular carcinoma with portal vein tumor thrombosis. *World journal of gastroenterology* **22**, 6851-6863, doi:10.3748/wjg.v22.i30.6851 (2016).

33 Prieto, J., Melero, I. & Sangro, B. Immunological landscape and immunotherapy of hepatocellular carcinoma. *Nature reviews. Gastroenterology & hepatology* **12**, 681-700, doi:10.1038/nrgastro.2015.173 (2015).

34 Hsu, C. S., Chao, Y. C., Lin, H. H., Chen, D. S. & Kao, J. H. Systematic Review: Impact of Interferon-based Therapy on HCV-related Hepatocellular Carcinoma. *Scientific reports* **5**, 9954, doi:10.1038/srep09954 (2015).

35 Saeki, I. *et al.* Effects of an oral iron chelator, deferasirox, on advanced hepatocellular carcinoma. *World journal of gastroenterology* **22**, 8967-8977, doi:10.3748/wjg.v22.i40.8967 (2016).

36 Bruix, J. *et al.* Regorafenib for patients with hepatocellular carcinoma who

progressed on sorafenib treatment (RESORCE): a randomised, double-blind, placebo-controlled, phase 3 trial. *Lancet (London, England)* **389**, 56-66, doi:10.1016/s0140-6736(16)32453-9 (2017).

37 Llovet, J. M. *et al.* Sorafenib in advanced hepatocellular carcinoma. *The New England journal of medicine* **359**, 378-390, doi:10.1056/NEJMoa0708857 (2008).

38 Abou-Alfa, G. K. *et al.* Phase Ib study of codrituzumab in combination with sorafenib in patients with non-curable advanced hepatocellular carcinoma (HCC). *Cancer chemotherapy and pharmacology* **79**, 421-429, doi:10.1007/s00280-017-3241-9 (2017).

39 Huynh, H. *et al.* RAD001 (everolimus) inhibits tumour growth in xenograft models of human hepatocellular carcinoma. *Journal of cellular and molecular medicine* **13**, 1371-1380, doi:10.1111/j.1582-4934.2008.00364.x (2009).

40 Finn, R. S. & Zhu, A. X. Targeting angiogenesis in hepatocellular carcinoma: focus on VEGF and bevacizumab. *Expert review of anticancer therapy* **9**, 503-509, doi:10.1586/era.09.6 (2009).

41 Kudo, M. *et al.* Ramucirumab as second-line treatment in patients with advanced hepatocellular carcinoma: Japanese subgroup analysis of the REACH trial. *Journal of gastroenterology* **52**, 494-503, doi:10.1007/s00535-016-1247-4 (2017).

42 Mazzanti, R., Arena, U. & Tassi, R. Hepatocellular carcinoma: Where are we? *World journal of experimental medicine* **6**, 21-36, doi:10.5493/wjem.v6.i1.21 (2016).

43 Tejeda-Maldonado, J. *et al.* Diagnosis and treatment of hepatocellular carcinoma: An update. *World journal of hepatology* **7**, 362-376, doi:10.4254/wjh.v7.i3.362 (2015).

44 Huang, L. Y. *et al.* Inhibition of Hec1 as a novel approach for treatment of primary liver cancer. *Cancer chemotherapy and pharmacology* **74**, 511-520, doi:10.1007/s00280-014-2540-7 (2014).

45 Frank-Kamenetsky, M. *et al.* Therapeutic RNAi targeting PCSK9 acutely lowers plasma cholesterol in rodents and LDL cholesterol in nonhuman primates. *Proceedings of the National Academy of Sciences of the United States of America* **105**, 11915-11920, doi:10.1073/pnas.0805434105 (2008).

46 Heyes, J., Palmer, L., Bremner, K. & MacLachlan, I. Cationic lipid saturation influences intracellular delivery of encapsulated nucleic acids. *Journal of controlled release : official journal of the Controlled Release Society* **107**, 276-287, doi:10.1016/j.jconrel.2005.06.014 (2005).

47 Snove, O., Jr. & Holen, T. Many commonly used siRNAs risk off-target activity. *Biochemical and biophysical research communications* **319**, 256-263, doi:10.1016/j.bbrc.2004.04.175 (2004).

48 Lv, H., Zhang, S., Wang, B., Cui, S. & Yan, J. Toxicity of cationic lipids and cationic polymers in gene delivery. *Journal of controlled release : official journal of the Controlled Release Society* **114**, 100-109, doi:10.1016/j.jconrel.2006.04.014 (2006).

49 Wei, Y., Mizzen, C. A., Cook, R. G., Gorovsky, M. A. & Allis, C. D. Phosphorylation of histone H3 at serine 10 is correlated with chromosome condensation during mitosis and meiosis in Tetrahymena. *Proceedings of the National Academy of Sciences of the United States of America* **95**, 7480-7484 (1998).

50 Huynh, H., Soo, K. C., Chow, P. K., Panasci, L. & Tran, E. Xenografts of human hepatocellular carcinoma: a useful model for testing drugs. *Clinical cancer research : an official journal of the American Association for Cancer Research* **12**, 4306-4314, doi:10.1158/1078-0432.ccr-05-2568 (2006).

51 Kim, W. R., Flamm, S. L., Di Bisceglie, A. M. & Bodenheimer, H. C. Serum activity of alanine aminotransferase (ALT) as an indicator of health and disease. *Hepatology (Baltimore, Md.)* **47**, 1363-1370, doi:10.1002/hep.22109 (2008).

52 Tentler, J. J. *et al.* Patient-derived tumour xenografts as models for oncology drug development. *Nature reviews. Clinical oncology* **9**, 338-350, doi:10.1038/nrclinonc.2012.61 (2012).

53 Pompili, L., Porru, M., Caruso, C., Biroccio, A. & Leonetti, C. Patient-derived xenografts: a relevant preclinical model for drug development. *Journal of experimental & clinical cancer research : CR* **35**, 189, doi:10.1186/s13046-016-0462-4 (2016).

54 Fichtner, I. *et al.* Establishment of patient-derived non-small cell lung cancer xenografts as models for the identification of predictive biomarkers. *Clinical cancer research : an official journal of the American Association for Cancer Research* **14**, 6456-6468, doi:10.1158/1078-0432.ccr-08-0138 (2008).

55 Wang, D. *et al.* Molecular heterogeneity of non-small cell lung carcinoma patient-derived xenografts closely reflect their primary tumors. *International journal of cancer* **140**, 662-673, doi:10.1002/ijc.30472 (2017).

56 Perez-Soler, R. *et al.* Response and determinants of sensitivity to paclitaxel in human non-small cell lung cancer tumors heterotransplanted in nude mice. *Clinical cancer research : an official journal of the American Association for Cancer Research* **6**, 4932-4938 (2000).

57 Daniel, V. C. *et al.* A primary xenograft model of small-cell lung cancer reveals irreversible changes in gene expression imposed by culture in vitro. *Cancer research* **69**, 3364-3373, doi:10.1158/0008-5472.can-08-4210 (2009).

58 Zhang, X. C. *et al.* Establishment of patient-derived non-small cell lung cancer

xenograft models with genetic aberrations within EGFR, KRAS and FGFR1: useful tools for preclinical studies of targeted therapies. *Journal of translational medicine* **11**, 168, doi:10.1186/1479-5876-11-168 (2013).

59 Ilie, M. *et al.* Setting up a wide panel of patient-derived tumor xenografts of non-small cell lung cancer by improving the preanalytical steps. *Cancer medicine* **4**, 201-211, doi:10.1002/cam4.357 (2015).

60 Owonikoko, T. K. *et al.* Patient-derived xenografts faithfully replicated clinical outcome in a phase II co-clinical trial of arsenic trioxide in relapsed small cell lung cancer. *Journal of translational medicine* **14**, 111, doi:10.1186/s12967-016-0861-5 (2016).

61 Nukatsuka, M. *et al.* Combination therapy using oral S-1 and targeted agents against human tumor xenografts in nude mice. *Experimental and therapeutic medicine* **3**, 755-762, doi:10.3892/etm.2012.484 (2012).

62 Hu, Y., Wang, L., Gu, J., Qu, K. & Wang, Y. Identification of microRNA differentially expressed in three subtypes of non-small cell lung cancer and in silico functional analysis. *Oncotarget* **8**, 74554-74566, doi:10.18632/oncotarget.20218 (2017).

63 Nicholson, A. G. *et al.* The International Association for the Study of Lung Cancer Lung Cancer Staging Project: Proposals for the Revision of the Clinical and Pathologic Staging of Small Cell Lung Cancer in the Forthcoming Eighth Edition of the TNM Classification for Lung Cancer. *Journal of thoracic oncology : official publication of the International Association for the Study of Lung Cancer* **11**, 300-311, doi:10.1016/j.jtho.2015.10.008 (2016).

64 Johnson, J. R. *et al.* Approval summary for erlotinib for treatment of patients with locally advanced or metastatic non-small cell lung cancer after failure of at least one prior chemotherapy regimen. *Clinical cancer research : an official journal of the American Association for Cancer Research* **11**, 6414-6421, doi:10.1158/1078-0432.ccr-05-0790 (2005).

65 Sequist, L. V. *et al.* First-line gefitinib in patients with advanced non-small-cell lung cancer harboring somatic EGFR mutations. *Journal of clinical oncology : official journal of the American Society of Clinical Oncology* **26**, 2442-2449, doi:10.1200/jco.2007.14.8494 (2008).

66 Dungo, R. T. & Keating, G. M. Afatinib: first global approval. *Drugs* **73**, 1503-1515, doi:10.1007/s40265-013-0111-6 (2013).

67 Malik, S. M. *et al.* U.S. Food and Drug Administration approval: crizotinib for treatment of advanced or metastatic non-small cell lung cancer that is anaplastic lymphoma kinase positive. *Clinical cancer research : an official journal of the*

American Association for Cancer Research **20**, 2029-2034, doi:10.1158/1078-0432.ccr-13-3077 (2014).

68 Kim, D. W. *et al.* Activity and safety of ceritinib in patients with ALK-rearranged non-small-cell lung cancer (ASCEND-1): updated results from the multicentre, open-label, phase 1 trial. *The Lancet. Oncology* **17**, 452-463, doi:10.1016/s1470-2045(15)00614-2 (2016).

69 Song, Z., Wang, M. & Zhang, A. Alectinib: a novel second generation anaplastic lymphoma kinase (ALK) inhibitor for overcoming clinically-acquired resistance. *Acta pharmaceutica Sinica. B* **5**, 34-37, doi:10.1016/j.apsb.2014.12.007 (2015).

70 Hazarika, M., White, R. M., Johnson, J. R. & Pazdur, R. FDA drug approval summaries: pemetrexed (Alimta). *The oncologist* **9**, 482-488, doi:10.1634/theoncologist.9-5-482 (2004).

71 Cohen, M. H., Gootenberg, J., Keegan, P. & Pazdur, R. FDA drug approval summary: bevacizumab (Avastin) plus Carboplatin and Paclitaxel as first-line treatment of advanced/metastatic recurrent nonsquamous non-small cell lung cancer. *The oncologist* **12**, 713-718, doi:10.1634/theoncologist.12-6-713 (2007).

72 Salgia, R. *et al.* A randomized phase II study of LY2510924 and carboplatin/etoposide versus carboplatin/etoposide in extensive-disease small cell lung cancer. *Lung cancer (Amsterdam, Netherlands)* **105**, 7-13, doi:10.1016/j.lungcan.2016.12.020 (2017).

73 Brahmer, J. *et al.* Nivolumab versus Docetaxel in Advanced Squamous-Cell Non-Small-Cell Lung Cancer. *The New England journal of medicine* **373**, 123-135, doi:10.1056/NEJMoa1504627 (2015).

74 Makita, Y. *et al.* Anti-tumor activity of KNTC2 siRNA in orthotopic tumor model mice of hepatocellular carcinoma. *Biochemical and biophysical research communications* **493**, 800-806, doi:10.1016/j.bbrc.2017.08.088 (2017).

75 Sato, T. *et al.* Long-term expansion of epithelial organoids from human colon, adenoma, adenocarcinoma, and Barrett's epithelium. *Gastroenterology* **141**, 1762-1772, doi:10.1053/j.gastro.2011.07.050 (2011).

76 Schneeberger, V. E., Allaj, V., Gardner, E. E., Poirier, J. T. & Rudin, C. M. Quantitation of Murine Stroma and Selective Purification of the Human Tumor Component of Patient-Derived Xenografts for Genomic Analysis. *PloS one* **11**, e0160587, doi:10.1371/journal.pone.0160587 (2016).

77 Taromi, S. *et al.* CXCR4 antagonists suppress small cell lung cancer progression. *Oncotarget* **7**, 85185-85195, doi:10.18632/oncotarget.13238 (2016).

78 Wu, G. *et al.* Small molecule targeting the Hec1/Nek2 mitotic pathway suppresses

tumor cell growth in culture and in animal. *Cancer research* **68**, 8393-8399, doi:10.1158/0008-5472.can-08-1915 (2008).

79 Hu, C. M. *et al.* Novel small molecules disrupting Hec1/Nek2 interaction ablate tumor progression by triggering Nek2 degradation through a death-trap mechanism. *Oncogene* **34**, 1220-1230, doi:10.1038/onc.2014.67 (2015).

80 Pollack, V. A. *et al.* Inhibition of epidermal growth factor receptor-associated tyrosine phosphorylation in human carcinomas with CP-358,774: dynamics of receptor inhibition in situ and antitumor effects in athymic mice. *The Journal of pharmacology and experimental therapeutics* **291**, 739-748 (1999).

81 Pao, W. *et al.* KRAS mutations and primary resistance of lung adenocarcinomas to gefitinib or erlotinib. *PLoS medicine* **2**, e17, doi:10.1371/journal.pmed.0020017 (2005).

82 Pao, W. *et al.* Acquired resistance of lung adenocarcinomas to gefitinib or erlotinib is associated with a second mutation in the EGFR kinase domain. *PLoS medicine* **2**, e73, doi:10.1371/journal.pmed.0020073 (2005).

83 Ekert, J. E. *et al.* Three-dimensional lung tumor microenvironment modulates therapeutic compound responsiveness in vitro--implication for drug development. *PloS one* **9**, e92248, doi:10.1371/journal.pone.0092248 (2014).

84 Friedrich, J., Seidel, C., Ebner, R. & Kunz-Schughart, L. A. Spheroid-based drug screen: considerations and practical approach. *Nature protocols* **4**, 309-324, doi:10.1038/nprot.2008.226 (2009).

85 Perche, F. & Torchilin, V. P. Cancer cell spheroids as a model to evaluate chemotherapy protocols. *Cancer biology & therapy* **13**, 1205-1213, doi:10.4161/cbt.21353 (2012).

86 Endo, H. *et al.* Spheroid culture of primary lung cancer cells with neuregulin 1/HER3 pathway activation. *Journal of thoracic oncology : official publication of the International Association for the Study of Lung Cancer* **8**, 131-139, doi:10.1097/JTO.0b013e3182779ccf (2013).

87 Onion, D. *et al.* 3-Dimensional Patient-Derived Lung Cancer Assays Reveal Resistance to Standards-of-Care Promoted by Stromal Cells but Sensitivity to Histone Deacetylase Inhibitors. *Molecular cancer therapeutics* **15**, 753-763, doi:10.1158/1535-7163.mct-15-0598 (2016).

88 Adams, D. *et al.* Patisiran, an RNAi Therapeutic, for Hereditary Transthyretin Amyloidosis. *The New England journal of medicine* **379**, 11-21, doi:10.1056/NEJMoa1716153 (2018).

89 Huang, L. Y. *et al.* Characterization of the biological activity of a potent small

molecule Hec1 inhibitor TAI-1. *Journal of experimental & clinical cancer research : CR* **33**, 6, doi:10.1186/1756-9966-33-6 (2014).

90 Zhu, Y. *et al.* Small Molecule TH-39 Potentially Targets Hec1/Nek2 Interaction and Exhibits Antitumor Efficacy in K562 Cells via G0/G1 Cell Cycle Arrest and Apoptosis Induction. *Cellular physiology and biochemistry : international journal of experimental cellular physiology, biochemistry, and pharmacology* **40**, 297-308, doi:10.1159/000452546 (2016).

91 Wei, R., Ngo, B., Wu, G. & Lee, W. H. Phosphorylation of the Ndc80 complex protein, HEC1, by Nek2 kinase modulates chromosome alignment and signaling of the spindle assembly checkpoint. *Molecular biology of the cell* **22**, 3584-3594, doi:10.1091/mbc.E11-01-0012 (2011).

92 Hu, P., Chen, X., Sun, J., Bie, P. & Zhang, L. D. siRNA-mediated knockdown against NUF2 suppresses pancreatic cancer proliferation in vitro and in vivo. *Bioscience reports* **35**, doi:10.1042/bsr20140124 (2015).

93 Cui, F., Hu, J., Fan, Y., Tan, J. & Tang, H. Knockdown of spindle pole body component 25 homolog inhibits cell proliferation and cycle progression in prostate cancer. *Oncology letters* **15**, 5712-5720, doi:10.3892/ol.2018.8003 (2018).

94 Penna, L. S., Henriques, J. A. P. & Bonatto, D. Anti-mitotic agents: Are they emerging molecules for cancer treatment? *Pharmacology & therapeutics* **173**, 67-82, doi:10.1016/j.pharmthera.2017.02.007 (2017).

95 Makita, Y. *et al.* Antitumor activity of kinetochore-associated protein 2 siRNA against lung cancer patient-derived tumor xenografts. *Oncology letters* **15**, 4676-4682, doi:10.3892/ol.2018.7890 (2018).